

## Zagazig Journal of Forensic Medicine and Toxicology

Journal homepage: <https://zjfm.journals.ekb.eg/>

### Original article

#### Evaluation of the Role of Carvacrol against Acetamiprid Induced Apoptosis and DNA Damage in Liver and Kidney of Adult Male Albino Rats

Nahla Mohamed Ibrahim <sup>1</sup>, Wesam Barakat Assy <sup>1</sup>, Samar R. Mohamed <sup>2</sup>, Samaa M El-Mahroky <sup>2</sup>, Hend sameh <sup>3</sup>, Elham El shawadfy Megahed <sup>\*1</sup>

<sup>1</sup> Forensic Medicine and Clinical Toxicology Department, Faculty of Medicine, Zagazig University, Zagazig, Egypt

<sup>2</sup> Medical Histology and Cell Biology Department, Faculty of Medicine, Zagazig University, Zagazig, Egypt

<sup>3</sup> Medical Biochemistry Department, Faculty of Medicine, Zagazig University, Zagazig, Egypt

### ARTICLE INFO

### Abstract

#### Article history

Received: 7- 3- 2024

Revised: 19- 4- 2024

Accepted: 22- 5- 2024

#### Keywords:

Carvacrol, acetamiprid, hepatotoxicity, nephrotoxicity, rats.

**Background:** Human Exposure to acetamiprid (ACP) is highly frequent because it is widely used insecticide. Acetamiprid has potential toxic health effects on liver and kidney that make it an issue of concern to public health. Carvacrol is an antioxidant and has therapeutic uses. **Aim:** This work was done to evaluate the Carvacrol protective role against highly toxic effects of acetamiprid produced biochemical, histo-pathological and immune-histochemical changes in liver and kidney of male albino rats. **Material and Methods:** Thirty-two adult male albino rats were divided into: Control group, carvacrol-treated, acetamiprid-treated, and carvacrol +acetamiprid treated group. By the end of the 4th week, 24 hours after the last dose, the following laboratory markers were measured: serum ALT, AST, Total bilirubin, Urea, uric acid, and Creatinine. Hepatic and renal tissue MDA, catalase and reduced glutathione. DNA fragmentation assay was done and DNA fragmentation visualized on gel electrophoresis in both hepatic and renal tissues. Histopathological study by H&E and Mallory trichome stain was done. Immunohistochemical staining by cleaved caspase 3 and iNOS were demonstrated. **Results:** In the acetamiprid treated group, there was increase in ALT, AST, total bilirubin, uric acid, Creatinine and Urea serum levels. Also, acetamiprid induced elevation in liver and kidney tissues MDA. Acetamiprid caused decrease in hepatic and renal tissue catalase and GSH. The DNA fragmentation assay detected increased DNA fragmentation in hepatic and renal tissues of the acetamiprid group and was lowered by Co-administration of carvacrol. Histopathology and Immunohistochemical staining showed that: Acetamiprid induced histological damages and strong immunoreaction decreased by co-treatment of carvacrol. **Conclusion:** Administration of carvacrol produced partial and incomplete improvement of liver and kidney function and histology beside an improvement in oxidative stress and inflammation caused by acetamiprid. **Recommendations:** Further studies are needed to investigate other protective substances against acetamiprid toxicity.

## INTRODUCTION

The emergence of new contaminants has caught people's attention nowadays. Neonicotinoids (NOEs) and organophosphate esters (OPEs) which are new replacements for pesticides or flame retardants, are regarded as low-risk contaminants for humans (*Zhang et al., 2023*). The most widely used pesticides in the neonicotinoid class are acetamiprid, nitenpyram, clothianidin, thiamethoxam, imidacloprid, and dinotefuran. Acetamiprid and imidaprid are two of the neonicotinoid insecticides that are most frequently employed. Neonicotinoids produce paralysis and hyper excitation in insects by preventing the passage of cholinergic impulses (*Sevim et al., 2023*).

Oxidative stress results from imbalance between free radicals production and the capacity of antioxidant system. Free radicals cause oxidative harm to several cell components (*Samarghandian et al., 2015*). Research suggests that taking natural antioxidant supplements improves an organ's ability to function when it is exposed to stressful conditions. Essential oils have demonstrated promising therapeutic effects against a variety of ailments in recent years (*Ahmadi et al., 2023*). Among the several liquid phenolic monoterpenoid with broad biological action found in the essential oils of the

Lamiaceae family, which includes oregano and thyme, is carvacrol (2-methyl-5-isopropyl phenol) (*Masyita et al., 2022*). Numerous therapeutic benefits of carvacrol have been reported by research conducted both in vivo and in vitro. Carvacrol's therapeutic uses as an antibacterial, anti-hepatotoxic, anti-inflammatory, anti-tumor, antioxidant and analgesic, which have been extensively studied (*Mahmoodi et al., 2019; Javed et al., 2021*).

Remarkably, Carvacrol has been demonstrated to have good physicochemical characteristics that can be used in pharmaceuticals. These characteristics of carvacrol and its molecular mechanisms suggest that it may have significant effects in prevention and inhibition of many diseases (*Javed et al. 2021*). Although carvacrol has shown some encouraging effects on inflammation in the past, further clinical and molecular data must be gathered. Our goal was to look at the beneficial effects of carvacrol on the kidney and liver when exposed to neonicotinoid insecticides.

Thus, the aim of this work was to evaluate the Carvacrol protective role against toxic effects of acetamiprid produced bio-chemical, histo-pathological and immune-histochemical changes in liver and kidney of male albino rats.

## I. MATERIAL AND METHODS

### Material

1. Carvacrol (Phenol, 2-methyl-5-(1-methylethyl)- Formula

C<sub>10</sub>H<sub>14</sub>O, MW 150, CAS# 499-75-2, was purchased from Al Abgi essential oil factory, Egypt in the form of pale yellow liquid with purity  $\geq 99\%$ .

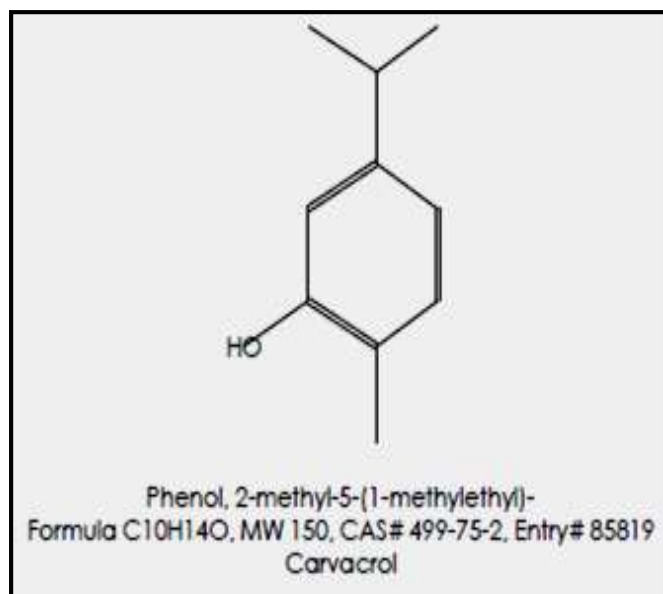


Figure (1): Chemical structure of carvacrol.

According to *Scalas et al. (2018)*, carvacrol was analyzed by gas chromatography-mass spectrometry (GC-MS) in Forensic Medicine and Clinical Toxicology Department, Faculty of Medicine, Zagazig University by professor doctor Laila Sabik.

Acetamidrid was purchased as Cetam commercial formulation containing 25% from a local Pesticide Manufacturing Co, Egypt.

Experimental design: Forty adult male albino rats weighing between 180 and 200 g. were taken from Zagazig University's Faculty of Medicine's animal house.

All rats underwent a 14-day passive prelamination phase before to the start of the experiment to help them acclimate to their new surroundings, assure their physical welfare, and keep sick animals out. Every rat in every cage received the same amount of food, and water was provided in distinct, hygienic containers. Throughout the trial, Rats were maintained in their enclosures under regular cycles of dark and light with a consistent temperature. The current investigation was carried out with consent from the Zagazig University IACUC Committee in Egypt and in compliance with international rules for animal research (ZU-IACUC/3 F/42/2023).

**Experimental protocol:** The whole period of the study was 4 weeks. Forty rats were divided as following:

**Group I (control group):** 16 rats were subdivided into two subgroups:

**Subgroup I a (Negative control group):**

There were 8 rats in it. To measure the baseline values of the examined parameters, each rat was given simply tap water and a standard diet.

**Subgroup Ib (Positive control group):**

There were eight rats in it. Distilled water (2mL) was administered to the rats once daily (as a vehicle).

**Group II (Carvacrol group):** It consisted of eight rats. Once daily, rats were given carvacrol dissolved in distilled water by oral gavage (50 mg/kg/day) for 4 weeks. Concentration was adjusted to yield a volume of 10 ml/kg (*Khalaf et al., 2021*).

**Group III (Acetamiprid group):** It consisted of eight rats. Each rat received 25 mg/kg/day i.e. (1/10 of LD50) Phogat et al., 2023) dissolved in distilled water by oral gavage for 4 weeks.

**Group IV (Carvacrol - Acetamiprid group):** It consisted of eight rats. Each rat was given carvacrol and acetamiprid by the same pervious mentioned doses. Carvacrol was given prior to acetamiprid as carvacrol exposure increased glutathione reductase expressions and cellular level of glutathione. (*Banik et al., 2019*). Carvacrol before tumor induction increased anti-oxidant enzymes such as catalase, superoxide dismutase, and glutathione levels, and restored the

histological lesions (*Arigesavan & Sudhandiran, 2015*).

**Methods:** Samples of blood were taken from the retro orbital plexus of anesthetized rats in all groups twenty-four hours after the end of therapy. The blood samples were spontaneously coagulated, and the separated serum was stored at  $-20^{\circ}\text{C}$  for further investigations. Then Liver and kidney were obtained and divided into 2 parts, the first part was used for making tissue homogenate for measuring oxidative stress biomarkers, DNA fragmentation assay and measurement of apoptosis genes. The second part was used for histopathological and immunohisto-chemical studies.

**Biochemical studies**

- 1- **Liver function tests:** ALT, AST and total bilirubin were estimated in serum as described in the manufacturer kits (Biodiagnostic, Cairo, Egypt ‘according to Reitman and Frankel, 1957).
- 2- **Kidney function tests:** serum urea, creatinine and uric acid were measured as described in the manufacturer kits (Biodiagnostic, Cairo, Egypt). Estimation of serum urea was carried out according to the modified Berthelot reaction (*Egwurugwu et al., 2018*). Estimation of serum Creatinine was carried out by fully automated COBAS

Integra 400+ clinical chemistry analyzer by compensated jaffe method (*Chauhan et al., 2017*).

**3- Lipid peroxidation and anti-oxidant markers:** levels of reduced glutathione (GSH), catalase (CAT) enzyme activity, and malondialdehyde (MDA) activity were estimated in tissue samples from the liver and kidney homogenates. The colorimetric method was used in accordance with the manufacturer's kit instructions (Biodiagnostic, Cairo, Egypt, catalase was assayed according to the method proposed by *Sinha, (1972)*, MDA was assayed according to the method proposed by *Ohkawa et al. (1979)*. Tissue GSH was assayed according to the method described by *Mannervik (1999)*.

#### 1- DNA Fragmentation Analysis:

DNA laddering was done in hepatic and renal tissues as shown by *Khalaf et al. (2021)*. To make tissue homogenates, tissue weighing no more than 25 mg was divided into small pieces in a 1.5 ml microcentrifuge tube. After that, 20 µl of Proteinase K and 180 µl of Buffer ATL were mixed by vortexing. Incubation at 56°C until fully lysed (1-3 hours). DNA was extracted by QIAamp DNA Mini Kit (Qiagen). The fragmented DNA electrophoretic patterns were examined on a 1.5% agarose gel that

had been stained with ethidium bromide and visualized under ultraviolet transillumination (Heralab GmbH laborgerate transilluminator, Germany) with 100 bp-Sizer™ DNA marker (iNtRON Biotechnology, Seongnam-si, Gyeonggi-do, 462-120, Korea) and photographed.

#### 2- mRNA Expression Levels of Apoptosis Genes

Gene expression analysis of Bax, Bcl-2 and p53 were examined by using Simply P Total RNA Extraction kit from Qiagen, Germany, catalogue No: Bsc52 S1 as previously described by *Öztaş et al. (2021)*. After total RNA extraction, cDNA was synthesized from isolated RNA by reverse transcription at 75°C for 5 min, 60°C for 60 min and 90°C for 5 min. (Maxime RT Premix kit catalogue no: 25081).

Quantitative Real-Time PCR was done by real-time cycler (DTlite 4 DNA-TECHNOLOGY). PCR was performed in a final volume of 20 µL containing 7µL of H<sub>2</sub>O, 1 µL of template DNA, 1 µL of each primer (1 µM), and 10µL of 2X PCR Master mix solution (Qiagen, Germany).

Table (1) contains the gene annealing temperatures and primer sequences.

The housekeeping gene, β-actin, and the apoptotic genes' specific cycle threshold (Ct)

for real-time PCR were identified, and the comparative Ct method was used to assess the relative expression.

Table (1): List the primers and associated annealing temperatures (Ta, °C) for the real-time PCR analysis of genes.

Paramet -ers	Primer (5'-3')	T a	
<b>Bax</b>	F: ACCAAGAAgCTgAgCgAgTATC	60	<i>Ali et al., 2017</i>
	R: ACAAAGATggTCACggTCTgCC		
<b>Bcl-2</b>	F: TgTggCCCAgATAggCACCCA	65	<i>Ali et al., 2017</i>
	R: ACTTCgCCgAgATgTCCAgCCA		
<b>p53</b>	F: AgAgTCTATAggCCCACCCC	61	<i>Ali et al., 2017</i>
	R: GCTCgACgCTAaggATCTgAC		
<b><math>\beta</math>-actin</b>	F: AACTACCTTCAACTCCAT	48	<i>Rosa et al., 2009</i>
	R: TgATCTTgATCTTCATTgTg		

### Histological study:

Light microscopic studies: Rats in all experimental groups had their liver and kidney fixed with formol saline 10% for 24 hours before being processed to create paraffin blocks. Cutting of 6  $\mu$ m thick paraffin sections mounting and staining by:

- Hematoxylin and Eosin stains (H&E) for studying the histological architecture.
- Mallory Trichrome stain for collagen fibers

demonstration (Bancroft and Gamble, 2008).

- Immunohistochemical staining:

According to *Sternberger (1986)*, the immunohistochemistry analyses for active caspase-3 (cell apoptosis marker) and iNOS (induced nitric oxide synthesis) protein expression (inflammatory marker) in hepatic and renal tissues were carried out.

Immunostaining required pretreatment, which was achieved by bringing the sections to a boil for 10 minutes in a 10 Mm, pH 6 citrate solution to retrieve the antigen. Following this, cooling of the sections were allowed for 20 minutes at room temperature. Subsequently, rabbit anti-caspase-3 (diluted to 1:1000, Abcam, Ltd.) and rabbit anti-iNOS (diluted to 1:100, Lab Vision Corporation, Fremont, California) were cultured with the sections. The sections were treated with the primary antibodies for an entire hour. The immunostaining procedure was done using an Ultravision detection system, and Mayer's hematoxylin was employed as a counterstain (*Suvarna et al., 2018*).

**Morphometric study:** It measures the mean area % for:

- Collagen fibers in sections with Mallory trichrome staining at a 400x magnification.

- iNOS immunoeexpression in sections with iNOS staining at a 400x magnification.
- Cleaved caspase-3 immunoeexpression in sections stained with caspase-3 at a 400x magnification.

For all measures, ten non-overlapping fields from different portions of the control group and all experimental groups were employed. Using a German-made Leica Microsystems LTD (DFC 295) software image analysis computer system, image analysis was performed in the Dentistry Research and Equipment Unit, Faculty of Dentistry, Cairo University.

**Statistical Analysis:** Version 26 of SPSS was used to examine the data. The Shapiro-Wilk test was employed to confirm the assumptions made for parametric testing. Standard deviations and means were used to characterize quantitative variables. For normally distributed data, a one-way ANOVA test was employed between two

groups to evaluate quantitative data. Fisher LSD comparison was performed to identify differences between each of the two separate groups where the differences were significant.  $P < 0.05$  was chosen as the level of statistical significance. If  $p \leq 0.001$  a highly significant difference was detected.

## II. RESULTS

In the present study, the comparison between the positive and negative control subgroups revealed statistically non-significant difference regarding all the studied biochemical, histological, immunohistochemical and histomorphometric studies. Therefore, we used the negative control group as a comparison marker for the other treated groups.

I-GC- MS analysis of carvacrol: One compound was identified by GC-MS analysis of carvacrol essential oil Phenol,2-methyl-5-(1-methylethyl)- as shown in table 2.

Table (2): Major compounds identified in carvacrol essential oil including their names, molecular formula, retention time, area percent, and molecular weight.

RT	Compound Name	Cas #	Area%	Molecular Formula	Molecular Weight	MF
47.88	Phenol,2-methyl-5-(1-methylethyl)	499-75-2	100.00	C10H14O	150	923
47.88	Phenol,2-methyl-5-(1-methylethyl)	499-75-2	100.00	C10H14O	150	923
47.88	Phenol,2-methyl-5-(1-methylethyl)	499-75-2	100.00	C10H14O	150	923

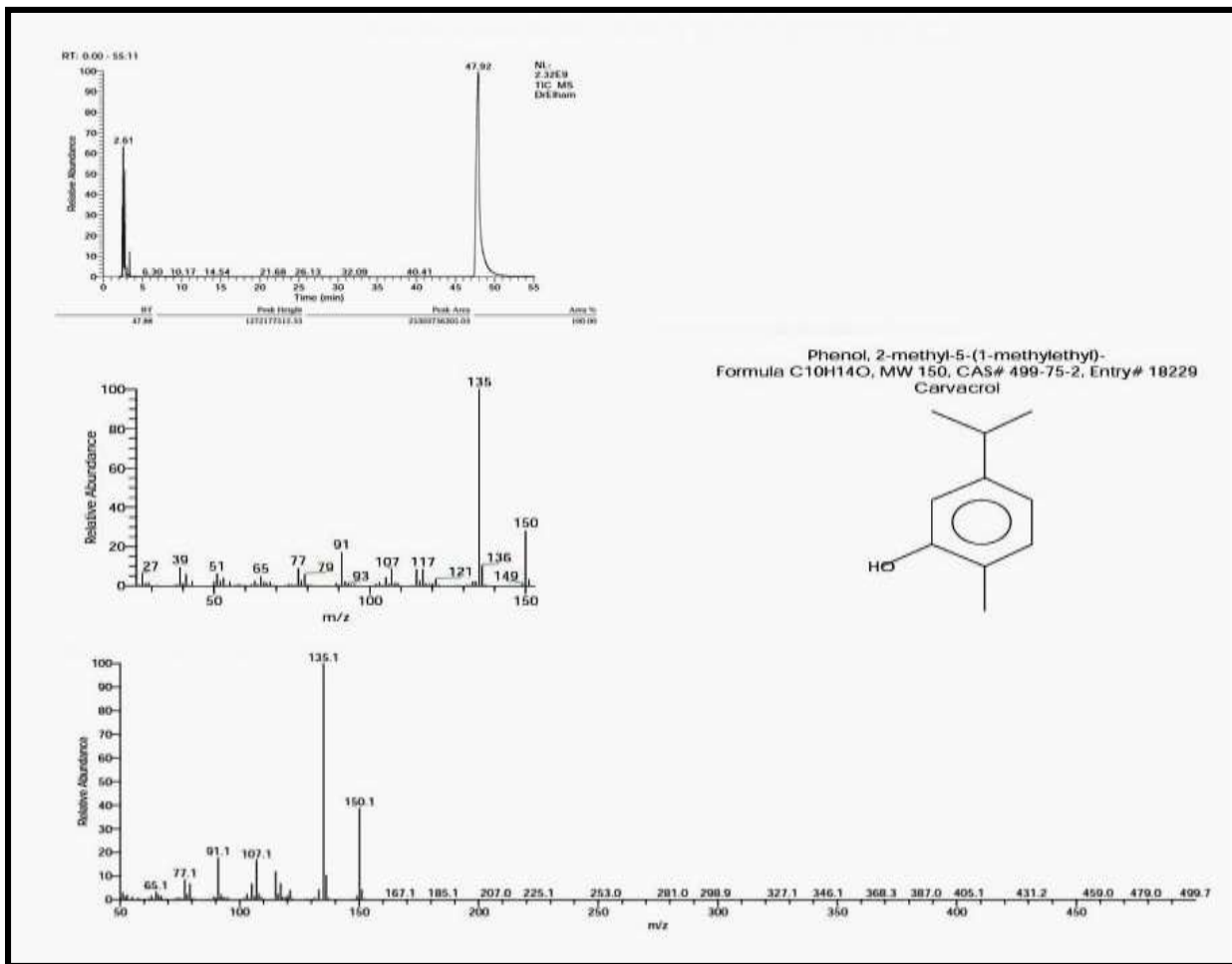


Figure (2): Total ionic chromatogram (GC-MS) of carvacrol essential oil.

## Biochemical Results

1. **Liver function test:** There was a statistically significant difference in the mean levels of ALT and AST across the several groups under investigation by ANOVA. The acetamiprid group's mean values increased significantly when compared to the negative control. Furthermore, carvacrol administration in carvacrol acetamiprid group led to a noteworthy reduction in their average values. Where there was no difference between the mean levels of ALT and AST in negative control group and the carvacrol group, the LSD comparison revealed a significant difference between each of the two individual groups. Regarding the mean values of total bilirubin, there was no difference between the various study groups (Table 3).
2. **Kidney function test:** A statistically significant variation was seen in the mean of uric acid, creatinine and urea across the several groups under investigation. In comparison to the negative control group, the acetamiprid group's mean values increased significantly. Furthermore, the administration of carvacrol in the carvacrol+acetamiprid group led to a noteworthy reduction in their average values. When comparing the mean values of uric acid, urea, and creatinine between the negative control group and the Carvacrol group, there was no statistically significant difference (Table 3). However, there was a significant difference between each of the two individual groups using LSD comparison.
3. **Lipid peroxidation and oxidative stress markers in liver and renal tissues:** Using ANOVA, There was significant difference between the different groups regarding the mean values of MDA, reduced glutathione and catalase enzyme in both liver and renal tissues. There was a high significant increase in the mean values of MDA and a high
4. **Significant decrease in the mean values of reduced glutathione and catalase enzyme in acetamiprid group when compared to negative control group.** Also, carvacrol administration in carvacrol +acetamiprid group resulted in
5. **Significant decrease in the mean values of MDA and significant increase in the mean values of reduced glutathione and catalase enzyme.** Using LSD comparison, the difference was significant between each two individual groups except when comparing negative control group and Carvacrol group where there was no statistically significant difference between the mean values of MDA, reduced glutathione and catalase enzyme

between them (Table 4)

6. DNA Fragmentation Assay: The hepatic and renal tissues from the acetamiprid-receiving group had the highest levels of DNA laddering, in the DNA fragmentation assay. However, there was no discernible change in DNA laddering between the carvacrol-receiving group and the negative control group. When compared to the acetamiprid-receiving group, co-administration of carvacrol and acetamiprid was able to reduce DNA fragmentation in the hepatic and renal tissues. The fragmented DNA's electrophoretic pattern on the agarose gel provided evidence for these conclusions

(Figure 3).

7. mRNA Expression Levels of Apoptosis Genes in liver and renal tissues: Using ANOVA, there was significant difference between the different groups regarding fold change in Bax, P53 and Bcl-2 in liver and renal tissues. On doing post hoc test, the difference is significant between each two

groups except when comparing negative control with carvacrol groups (Table 5).

Table (3): Comparison between groups regarding liver and kidney function tests

Parameters	Negative Control group	Carvacrol group	Acetamiprid group	Carvacrol +Acetamiprid group	F	p
	Mean $\pm$ SD					
ALT (U/l)	28.63 $\pm$ 2.72	29.88 $\pm$ 1.46 <sup>#</sup>	56.63 $\pm$ 5.34 <sup>a</sup>	38.38 $\pm$ 2.45 <sup>ab</sup>	121.106	<0.001**
AST (U/l)	11.38 $\pm$ 2.13	11.75 $\pm$ 2.44 <sup>#</sup>	28.63 $\pm$ 3.66 <sup>a</sup>	19.38 $\pm$ 2.33 <sup>ab</sup>	71.907	<0.001**
Total bilirubin (mg/dl)	0.27 $\pm$ 0.04	0.34 $\pm$ 0.19	0.37 $\pm$ 0.05	0.32 $\pm$ 0.02	1.233	0.316
Uric acid (mg/dl)	1.89 $\pm$ 0.29	1.91 $\pm$ 0.21 <sup>#</sup>	3.57 $\pm$ 0.87 <sup>a</sup>	2.79 $\pm$ 0.32 <sup>ab</sup>	20.926	<0.001**
Creatinine (mg/dl)	0.57 $\pm$ 0.07	0.52 $\pm$ 0.04 <sup>#</sup>	0.86 $\pm$ 0.07 <sup>a</sup>	0.65 $\pm$ 0.07 <sup>*b</sup>	42.792	<0.001**
Urea (mg/dl)	18.63 $\pm$ 2.13	19.13 $\pm$ 1.13 <sup>#</sup>	34.25 $\pm$ 5.6 <sup>a</sup>	22.88 $\pm$ 2.48 <sup>*b</sup>	39.084	<0.001**

Test used is ANOVA and Post Hoc test. F: One way ANOVA test, #p>0.05, \*p<0.05, ap<0.001 when compared to negative control group, bp<0.001 when compared to acetamiprid group.

Table (4): Comparison between groups regarding lipid peroxidation and oxidative stress markers in liver and renal tissues

Parameters	Negative Control group	Carvacrol group	Acetamiprid group	Carvacrol +Acetamiprid group	F	p
	Mean $\pm$ SD					
MDA (liver tissue)	451.25 $\pm$ 62.44	417.5 $\pm$ 23.15 <sup>#</sup>	837.88 $\pm$ 61.19 <sup>a</sup>	566.25 $\pm$ 37.39 <sup>ab</sup>	121.357	<0.001**
MDA (renal tissue)	433.75 $\pm$ 66.75	416.25 $\pm$ 17.47 <sup>#</sup>	828.88 $\pm$ 57.19 <sup>a</sup>	568.5 $\pm$ 33.88 <sup>ab</sup>	126.613	<0.001**
Reduced glutathione (liver tissue)	53.75 $\pm$ 6.8	66.38 $\pm$ 3.82 <sup>#</sup>	27.63 $\pm$ 4.37 <sup>a</sup>	48.38 $\pm$ 3.74 <sup>*b</sup>	88.825	<0.001**
Reduced glutathione (renal tissue)	53.38 $\pm$ 8.67	50.38 $\pm$ 6.26 <sup>#</sup>	27.63 $\pm$ 5.15 <sup>a</sup>	65.38 $\pm$ 3.46 <sup>ab</sup>	52.076	<0.001**
Catalase enzyme (liver tissue)	188.5 $\pm$ 15.31	197.75 $\pm$ 10.36 <sup>#</sup>	98.63 $\pm$ 10.84 <sup>a</sup>	151.38 $\pm$ 6 <sup>*b</sup>	130.901	<0.001**
Catalase enzyme (renal tissue)	185.63 $\pm$ 12.46	197.38 $\pm$ 8.54 <sup>#</sup>	98 $\pm$ 15.37 <sup>a</sup>	150.63 $\pm$ 6.32 <sup>ab</sup>	126.246	<0.001**

Test used is ANOVA and Post Hoc test (LSD). F: One way ANOVA test, #p>0.05, \*p<0.05, ap<0.001 when compared to negative control group, bp<0.001 when compared to acetamiprid group

Table (5) Comparison between groups regarding fold change of Bax, Bcl-2 and P53 in liver and renal tissues

Parameters	Negative Control group	Carvacrol group	Acetamiprid group	Carvacrol +acetamiprid group	F	P
	Mean $\pm$ SD					
Bax (liver tissue)	1.04 $\pm$ 0.13	1.33 $\pm$ 0.34 <sup>#</sup>	4.84 $\pm$ 0.25 <sup>a</sup>	1.98 $\pm$ 0.7 <sup>ab</sup>	141.93	<0.001**
Bax (renal tissue)	1.01 $\pm$ 0.24	1.03 $\pm$ 0.14 <sup>#</sup>	4.71 $\pm$ 0.68 <sup>a</sup>	2.19 $\pm$ 0.83 <sup>ab</sup>	78.356	<0.001**
Bcl-2 (liver tissue)	1.01 $\pm$ 0.06	0.84 $\pm$ 0.11 <sup>#</sup>	0.69 $\pm$ 0.15 <sup>a</sup>	0.91 $\pm$ 0.02 <sup>*b</sup>	15.771	<0.001**
Bcl-2 (renal tissue)	1.02 $\pm$ 0.14	0.86 $\pm$ 0.08 <sup>#</sup>	0.71 $\pm$ 0.14 <sup>a</sup>	0.89 $\pm$ 0.03 <sup>ab</sup>	19.158	<0.001**
P53 (liver tissue)	0.92 $\pm$ 0.14	1.12 $\pm$ 0.26 <sup>#</sup>	3.82 $\pm$ 1.2 <sup>a</sup>	1.93 $\pm$ 0.42 <sup>*b</sup>	33.027	<0.001**
P53 (renal tissue)	1.11 $\pm$ 0.25	1.05 $\pm$ 0.21 <sup>#</sup>	4.58 $\pm$ 0.68 <sup>a</sup>	1.78 $\pm$ 0.85 <sup>*b</sup>	69.338	<0.001**

Test used is ANOVA and Post Hoc test. F: One way ANOVA test, #p>0.05,\*p<0.05,ap<0.001 when compared to negative control group, bp<0.001 when compared to acetamiprid group

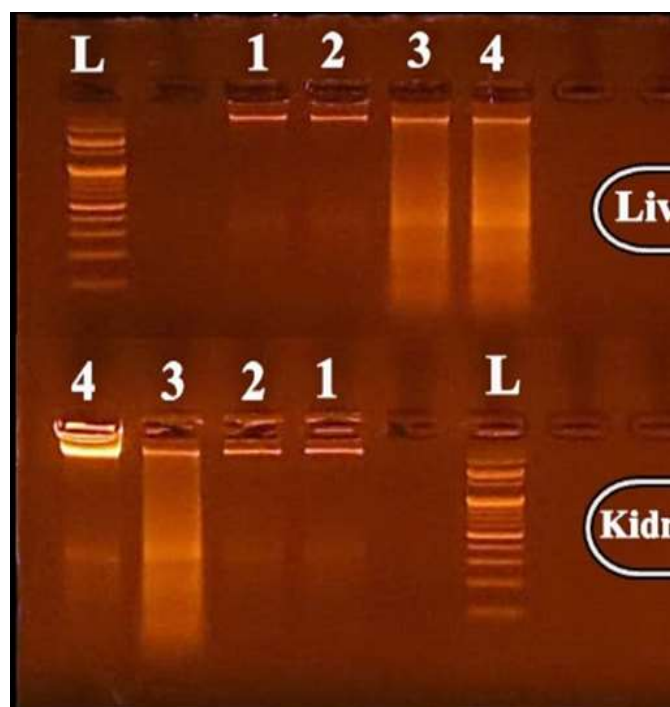


Figure 3: Agarose gel electrophoresis representing DNA fragmentation isolated from liver and kidney tissues. In DNA isolated from liver Lane L: 100-bp DNA ladder; lane 1: DNA from negative control group; lane 2: DNA from carvacrol group; lane 3: DNA from carvacrol+ acetamiprid group; lane 4: DNA from acetamiprid group. In DNA isolated from kidney Lane L: 100-bp DNA ladder; lane 1: DNA from negative control group; lane 2: DNA from carvacrol group; lane 3: DNA from acetamiprid group; lane 4: DNA from carvacrol + acetamiprid group.

**Histological results:****H&E staining results:****H&E staining of renal cortex of different studied groups:**

Negative control group showed normal renal cortex architecture; the glomerulus surrounded by Bowman's capsule. The renal tubules; proximal and distal convoluted tubules are observed (Figure4A). A section of Acetamiprid group showing disturbed structure of renal cortex; the glomeruli are congested with obliteration of bowman's space. Massive interstitial hemorrhage and severe inflammatory cellular infiltration are obvious. The tubules had deep acidophilic cytoplasm and shedded cellular debris in their lumen (Figure4B). Another section of the same group showing marked degenerative changes. Congested glomerulus and interstitial hemorrhage are noticed. Areas of complete tissue necrosis are noticed. Some tubules show degeneration while others show extensive vacuolations with numerous dark stained nuclei (Figure4C). A section from carvacrol+acetamiprid group showing improvement in the histological picture, most of the tubules are apparently normal however, minimal vacuolations and some dark stained nuclei are still present. Residual minimal glomerular congestion and interstitial hemorrhage are also still present (Figure4D).

**H&E staining of hepatic tissue of different studied groups:**

Negative control group showed normal histological structure of liver parenchyma, hepatocytes are polygonal with vesicular central nucleus and acidophilic cytoplasm. Some are binucleated. The hepatocytes arranged in cords radiating from central vein and separated by blood sinusoids lined by flat endothelium. Kuepfer cells are noticed in the sinusoids (Figure5A). Section from acetamiprid group showing disorganization of the histological structure, hepatocytes lost their normal arrangement and showed extensive vacuolations with dark stained nuclei. The central vein is dilated and congested. Inflammatory cellular infiltrations are present, areas of tissue necrosis and extravasation of blood. Some hepatocytes lost their boundaries (Figure5 B&C). Section from acetamiprid+carvacrol group showing improvement of the histological structure, the hepatocytes are polygonal with acidophilic cytoplasm and vesicular nuclei but some dark stained nuclei are still present. Residual congestion of the central vein and sinusoids is noticed (Figure 5D).

Negative control group showed the typical histological configuration of the portal region, Vesicular nuclei and acidophilic cytoplasm characterise polygonal hepatocytes. Some are

binucleated (Figure 6A). Section from acetamiprid group showing increased connective tissue deposition with inflammatory cell infiltrations in the portal region structures. The portal vein shows marked dilatation and congestion. The hepatic artery dilated and congested. The bile ducts show marked proliferation. Dilated congested blood sinusoids. Many hepatocytes show cytoplasmic vacuolations and dark stained nuclei (Figure 6B&C). Section from carvacrol+acetamiprid group showing improvement of the histological structure, of the portal area with residual duct proliferation and mild cellular infiltration. Most hepatocytes appear normal except for some dark stained nuclei (Figure 6D)

#### **Mallory trichrome staining results:**

#### **Mallory trichrome stained renal tissue of different studied groups showed:**

Collagen fibers around glomeruli and tubules were few in the negative control group (Figure7a). Collagen fibers were excessively deposited around blood vessels and tubules in the acetamiprid group (Figure7b). Collagen fiber deposition surrounding tubules and glomeruli was mild in the carvacrol+acetamiprid group (Figure 7c).

#### **Mallory trichrome stained hepatic tissue of different studied groups showed:**

Collagen fibers surrounding central vein (Figure 8a) and around portal area (Figure 8b) are few in the negative control group. The collagen fibers around central vein, in between the hepatocytes, (Figure 8c) and around portal area (Figure 8d) were excessively deposited in the acetamiprid group. Collagen fibers are slightly deposited around central vein (Figure 8e) and in the portal area (Figure 8f) in the carvacrol +acetamiprid group.

#### **Immunohistochemical staining results:**

#### **I. iNOS immunohistochemical staining results:**

Kidney sections of different studied groups showing iNOS immuno-histochemical reaction: Negative control group showed weak iNOS reaction among glomerular capillaries and few tubules (Figure9a). Acetamiprid group showed strong positive iNOS reaction in multiple renal tubules (Figure9b). carvacrol +Acetamiprid group showed mild positive iNOS reaction among some tubules (Figure9c).

Liver sections of different studied groups showing iNOS immuno-histochemical reaction: Negative control group showed weak positive cytoplasmic reaction in hepatocytes in liver sections (Figure10a). Strong positive reaction was observed in almost all the hepatocytes in the sections of the Acetamiprid group (Figure10b). Carvacrol+Acetamiprid group showed mild positive iNOS reaction among some

hepatocytes (Figure10c).

## II. Cleaved caspase-3 immunohistochemical staining results:

- Kidney sections of different studied groups showing cleaved caspase-3 immunohistochemical reaction: Negative control group shows few cleaved caspase 3 positive nuclei in few tubules (Fig.11a). Acetamiprid group shows numerous cleaved caspase-3 positive nuclei in most renal tubules (Figure11b). Carvacrol+Acetamiprid group shows some positive cleaved caspase3 nuclei among some tubules (Figure11c).
- Liver sections of different studied groups showing cleaved caspase-3 immunohistochemical reaction: Negative control group shows only few positive reactions of cleaved caspase3. positive nuclei of few hepatocytes (Figure12a). Acetamiprid group shows numerous positive nuclei to cleaved caspase-3 in most hepatocytes (Figure12b). carvacrol +Acetamiprid group shows some positive cleaved caspase3 nuclei among some hepatocytes (Figure12c).

### Morphometric results:

- The area percentage of collagen fibers was significantly higher in the acetamiprid group compared to the negative control; however, it was significantly lower in the carvacrol + acetamiprid group in kidney sections (Figure7d) and in liver sections (Figure8g).

- The mean area percent of iNOS immunopositive cells increased in a highly statistically significant way when comparing the acetamiprid group to the negative control group. In comparison to the acetamiprid group, carvacrol + acetamiprid significantly reduced the mean area percent of iNOS immunopositive cells in kidney sections (Figure9d) and in liver sections (Figure 10d).
- The mean area percentage of cleaved caspase-3 immunopositive cells increased significantly in the acetamiprid group compared to the negative control group. The mean area percent of cleaved caspase-3 immunopositive cells in kidney sections (Figure11d) and in liver sections (Figure12d) was considerably lower in the carvacrol +acetamiprid group as compared to the acetamiprid group.

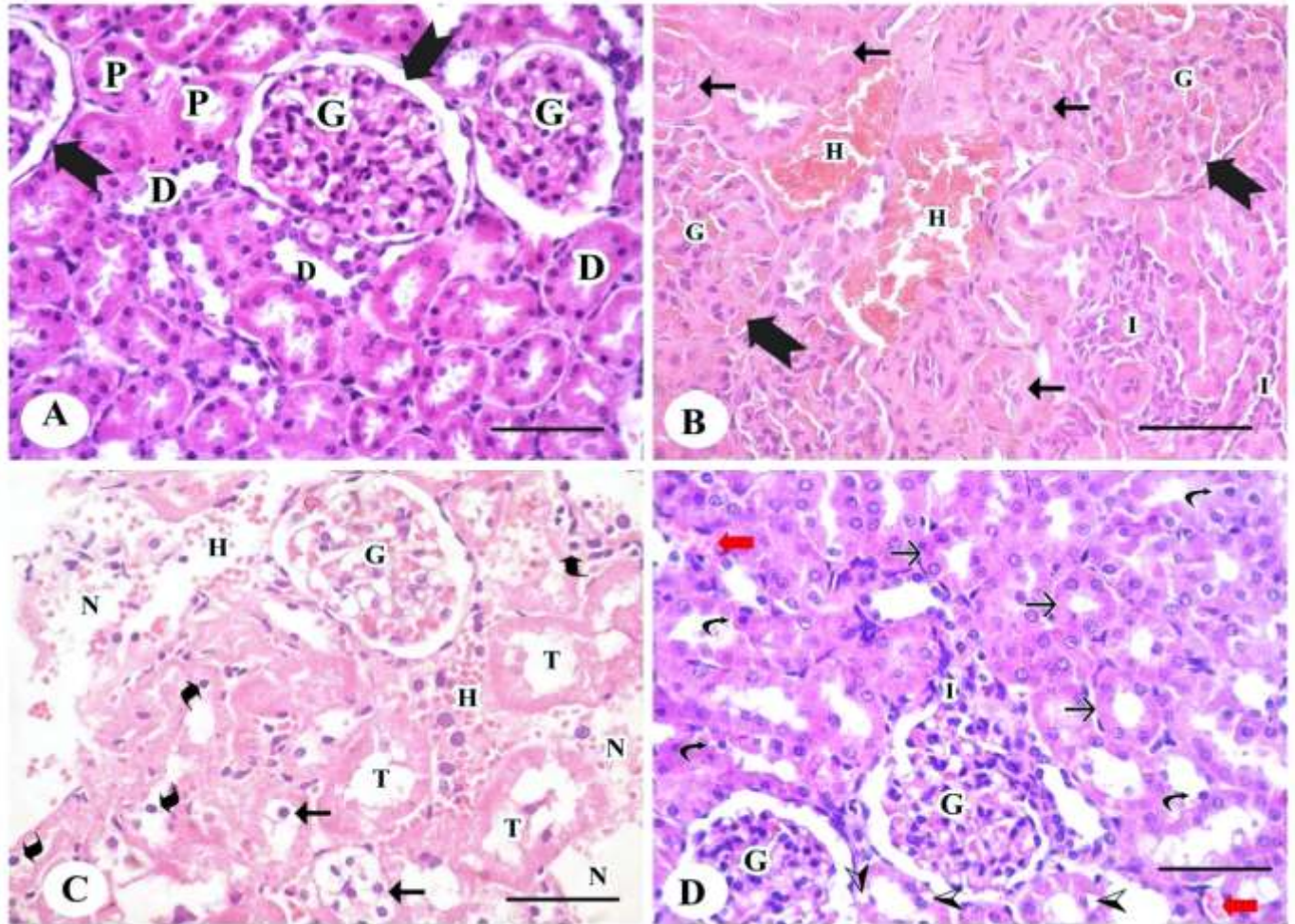


Figure 4: Haematoxylin and eosin-stained sections of the kidney cortex of different studied groups: The negative control group (A) showing normal renal cortex architecture; the glomerulus (G) surrounded by bowman's capsule (notched arrow). The renal tubules; proximal (P) and distal (D) convoluted tubules are observed. Acetamidrid-group (B) showing congested glomeruli (G) with obliteration of bowman's space (notched arrow). Massive interstitial haemorrhage (H) and severe inflammatory cellular infiltration (I) are obvious. The tubules (arrows) had deep acidophilic cytoplasm and shedded cellular debris in their lumen. Acetamidrid-group (C) showing areas of complete tissue necrosis (N) are noticed. Some tubules show degeneration (T) while others show extensive vacuolations (arrows) with numerous dark stained nuclei (curved arrows). Congested glomerulus (G) and interstitial haemorrhage (H) are also noticed. Carvacrol +Acetamidrid group (D) showing apparently normal tubules (T) however, minimal vacuolations (arrowheads) and some dark stained nuclei (curved arrows) are still present. Residual minimal glomerular congestion (G) and interstitial haemorrhage (red arrows) are also still present. (H&E x 400, scale bar 40µm).

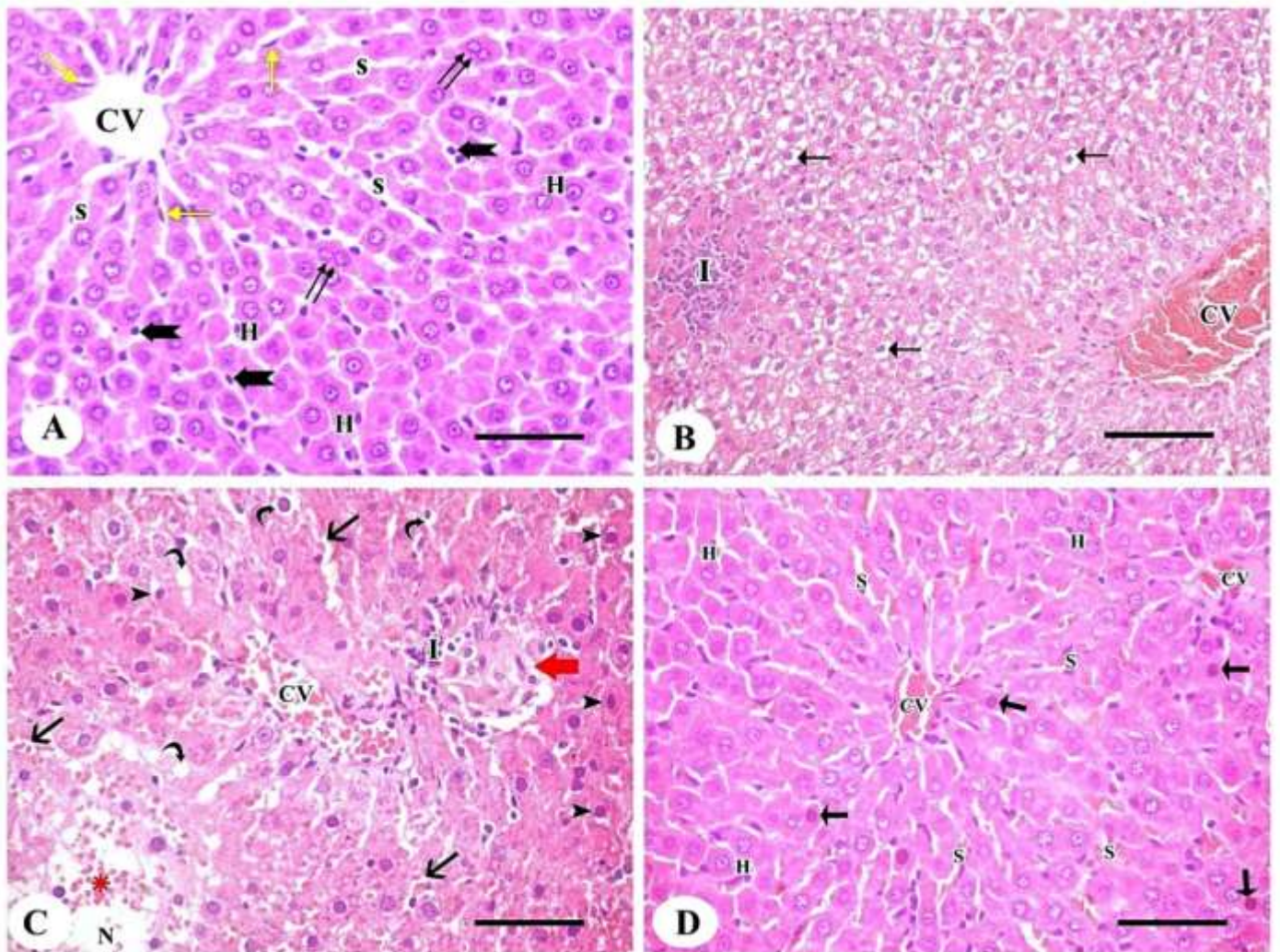


Figure 5: Hematoxylin & eosin-stained sections of liver tissue from different studied groups: The negative control group (A) showing normal hepatic parenchyma, hepatocytes (H) are polygonal with vesicular central nucleus and acidophilic cytoplasm. Some are binucleated (double arrows). The hepatocytes arranged in cords radiating from central vein (CV) and separated by blood sinusoids (S) lined by flat endothelium (yellow arrow). Kupfer cells (notched arrow) are noticed in the sinusoids (s). The acetaminophen group (B) showing that hepatocytes (H) lose their normal arrangement and show extensive vacuolations with dark stained nuclei (arrows). The central vein (CV) is dilated and congested. Inflammatory cellular infiltrations (I) are present. The acetaminophen group (C) showing area of tissue necrosis (N) and blood extravasation (asterisks). Some hepatocytes show dark stained nuclei (arrowheads), others loss of their boundaries (red arrow). Some vacuolations (curved arrow) and inflammatory cellular infiltrations (I) can be noticed. Dilated congested central vein (CV) and sinusoids (arrows) are noticed. Carvacrol + Acetaminophen group (D) showing almost normal hepatocytes (H). Some dark stained nuclei (arrows) are still present. Residual congestion of the central vein (CV) and sinusoids (s) is noticed. (H&E x 400, scale bar 40 $\mu$ m).

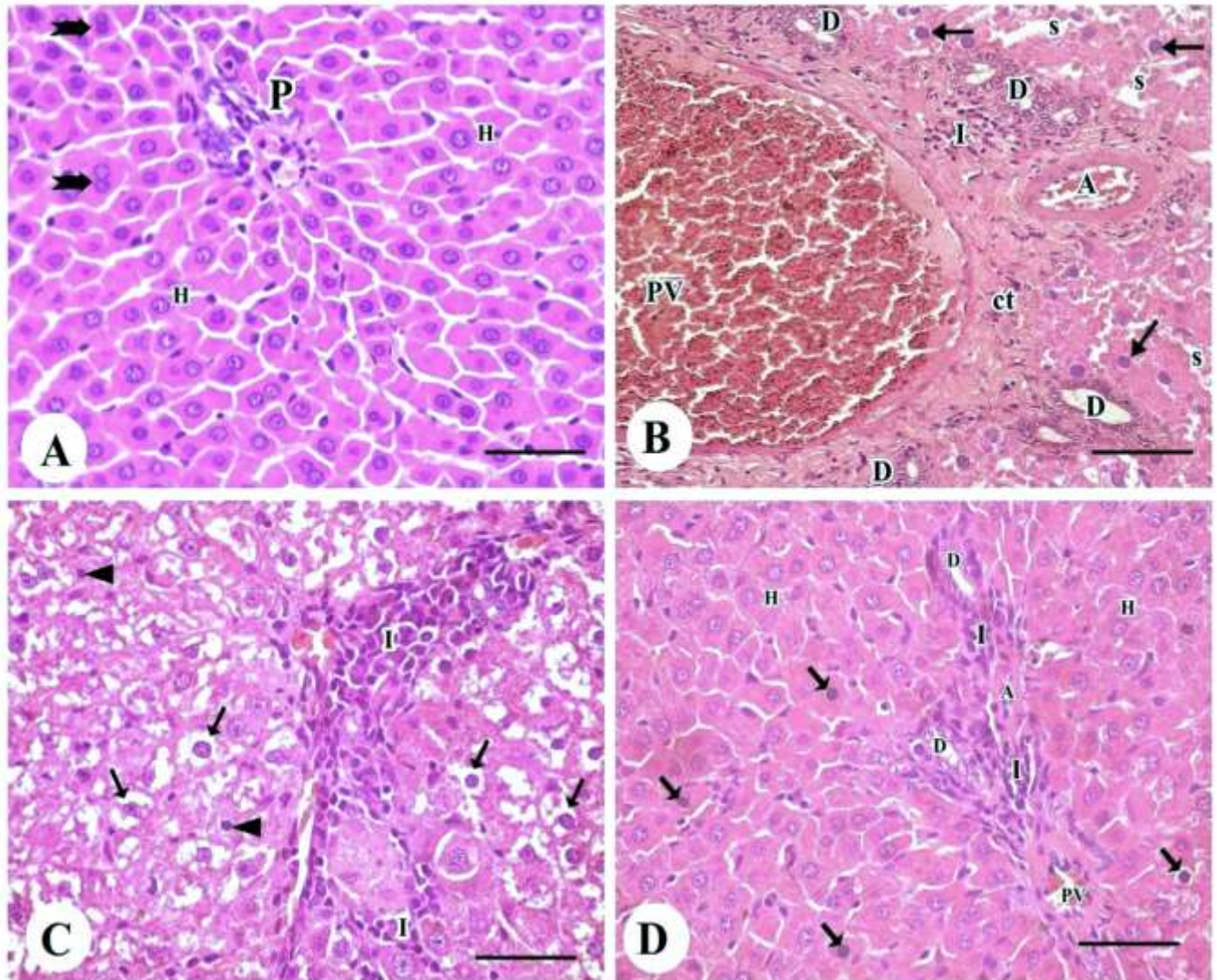


Figure 6: Hematoxylin & eosin-stained sections of portal area of liver from different studied groups: The negative control group(A) showing normal histological structure of portal area (P), hepatocytes (H) are polygonal with vesicular nucleus and acidophilic cytoplasm. Some are binucleated (notched arrows). The Acetamidrid group ( B) showing increased connective tissue (ct) deposition in the structures of portal area with inflammatory cellular infiltrations (I). The portal vein (PV) shows marked dilatation and congestion. The hepatic artery (A) dilated and congested. The bile ducts (d) show marked proliferation. Dilated congested blood sinusoids (s) and dark stained nuclei of the hepatocytes (arrows) are also observed. The Acetamidrid group (C)showing extensive inflammatory cellular infiltration (I) in the portal area. Many hepatocytes show cytoplasmic vacuolations (arrows) and dark stained nuclei (arrowheads). Carvacrol +Acetamidridgroup(D) showing improvement of the portal area with residual duct proliferation (D) and mild cellular infiltration (I). most hepatocytes (H) appear normal except for some dark stained nuclei (arrows). (H&E x 400, scale bar 40µm).

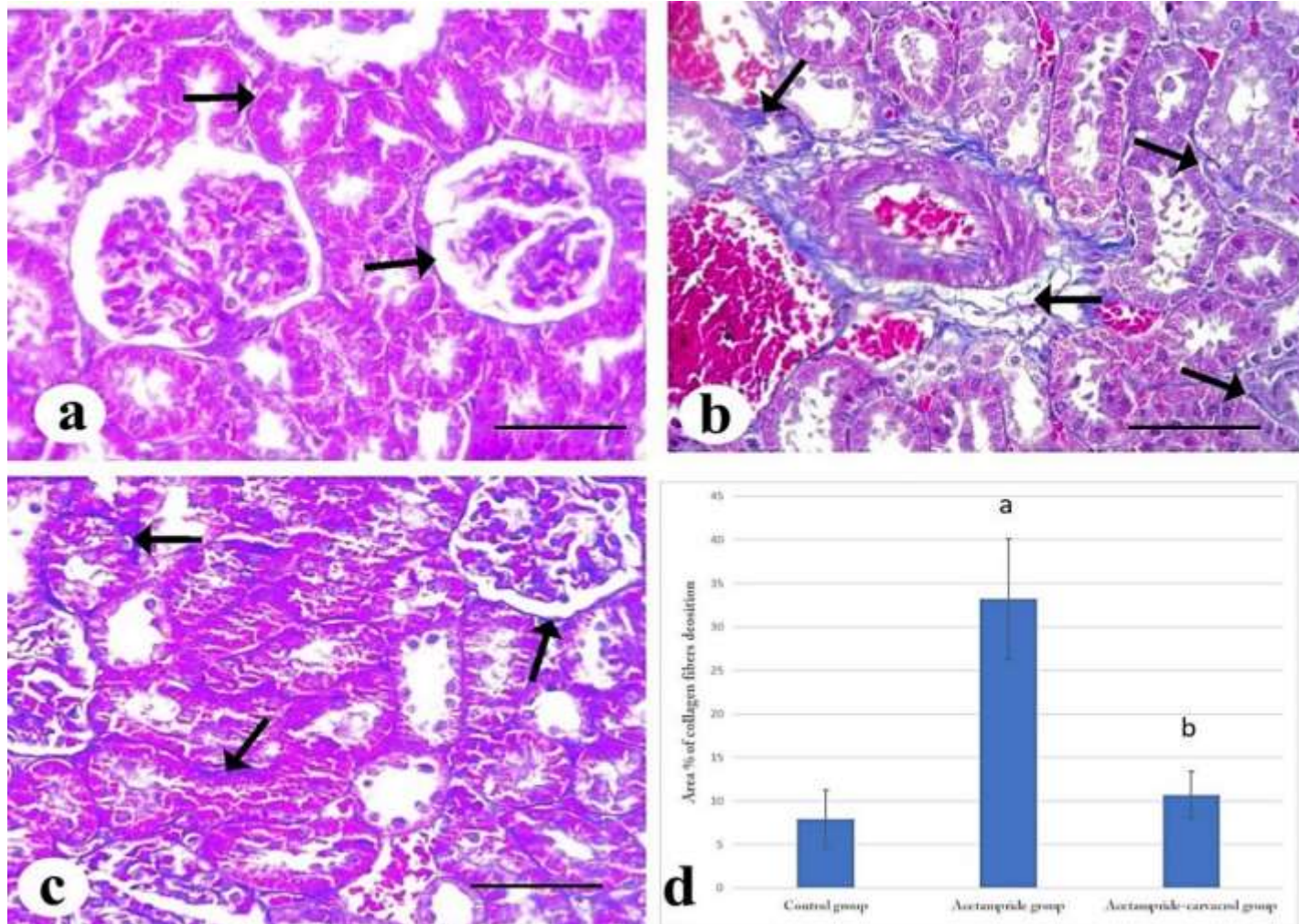


Figure 7: Mallory trichrome stained sections of different studied groups showing: Negative control group(a) shows minimal amount of collagen fibers around glomeruli and tubules (arrow). Acetamiprid group (b) showing excessive deposition of collagen fibers around blood vessels and tubules (arrow). Carvacrol +Acetamiprid group(c) shows mild deposition of collagen fibers around tubules and glomeruli (arrow) (MTC X 400, scale bar 40µm). d. Comparison between area % of collagen fibers deposition in different studied groups, a high significant difference with negative control group, b high significant difference with Acetamiprid group.

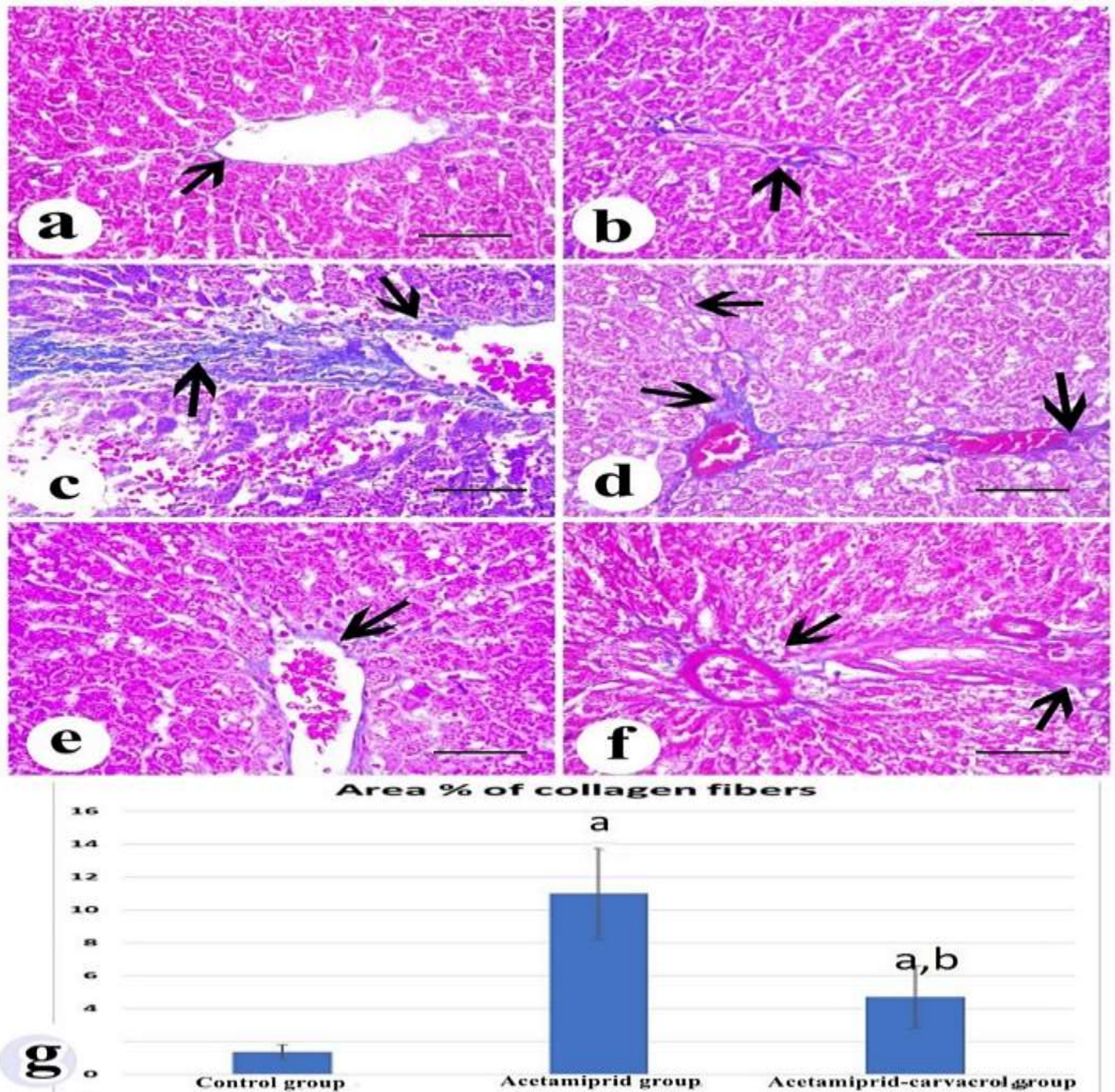


Figure 8: Mallory trichrome stained sections of different studied groups showing: (a & b) negative control group (a) shows minimal amount of collagen fibers around the central vein (arrow). Group b. shows minimal amount of collagen fibers around the portal area (arrow). Acetamiprid group (c) showing excessive deposition of collagen fibers around the central vein and in between hepatocytes (arrow). Group (d) showing increased deposition of collagen fibers in the portal area and in between hepatocytes (arrow). carvacrol + Acetamiprid group (e) shows mild deposition of collagen fibers around central vein (arrow). Acetamiprid-carvacrol group (f) shows mild deposition of collagen fibers in the portal area (arrow) (MTC X 400, scale bar 40µm). g. Comparison between area % of collagen fibers deposition in different studied groups, a high significant difference with control group, b high significant difference with Acetamiprid group.

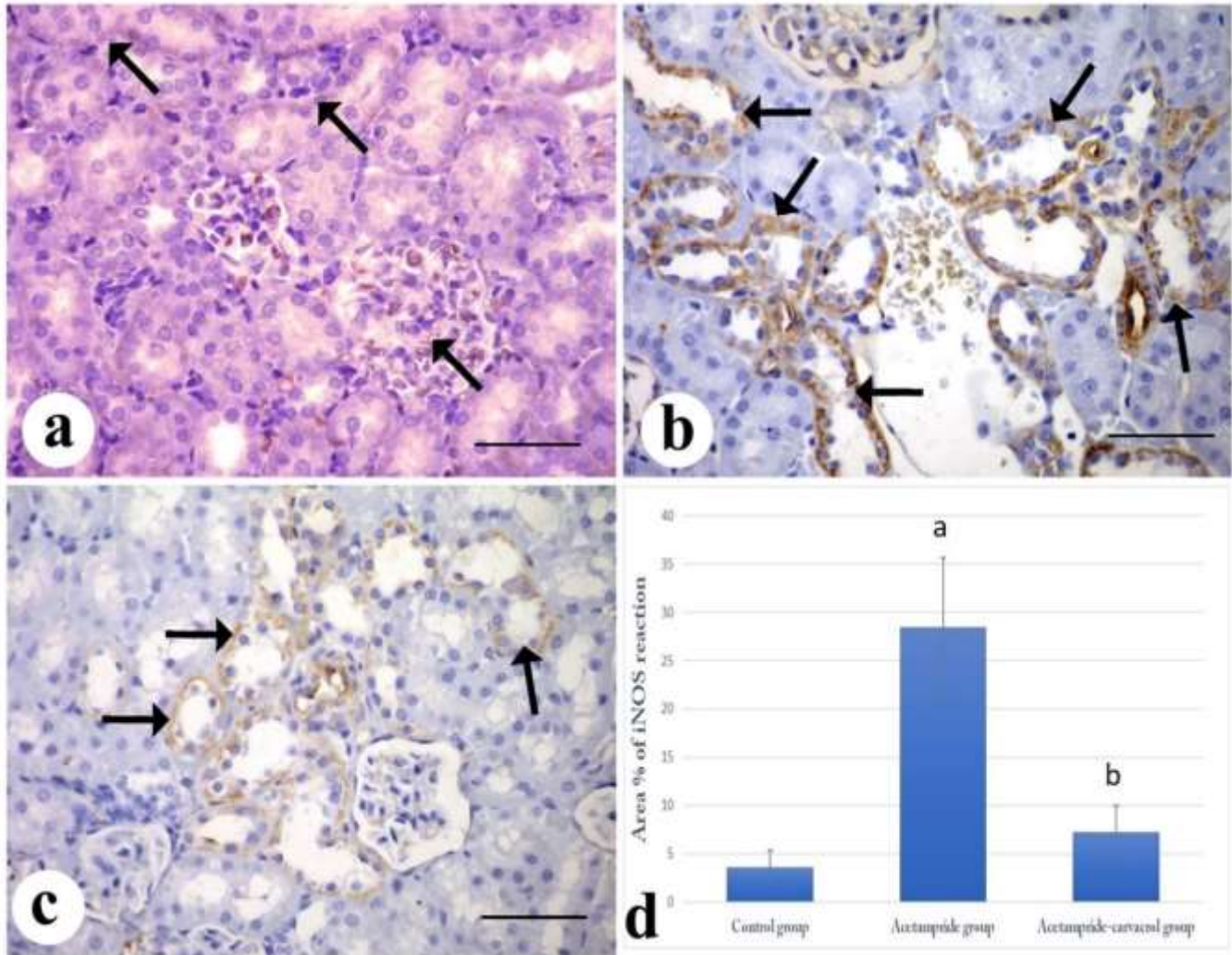


Figure 9: Sections of different studied groups showing iNOS immunohistochemical reaction: negative control group(a) shows weak iNOS reaction among glomerular capillaries and few tubules (arrows). Acetamipride group (b) shows strong positive iNOS reaction in multiple renal tubules (arrows). Carvacrol + Acetamiprid group(c) shows mild positive iNOS reaction among some tubules (arrows) (Immune peroxidase technique for iNOS x 400, scalebar 40 $\mu$ m). d. Comparison between area % of iNOS immunoreactions in different studied groups, a high significant difference with control group, b high significant difference with Acetamiprid group.

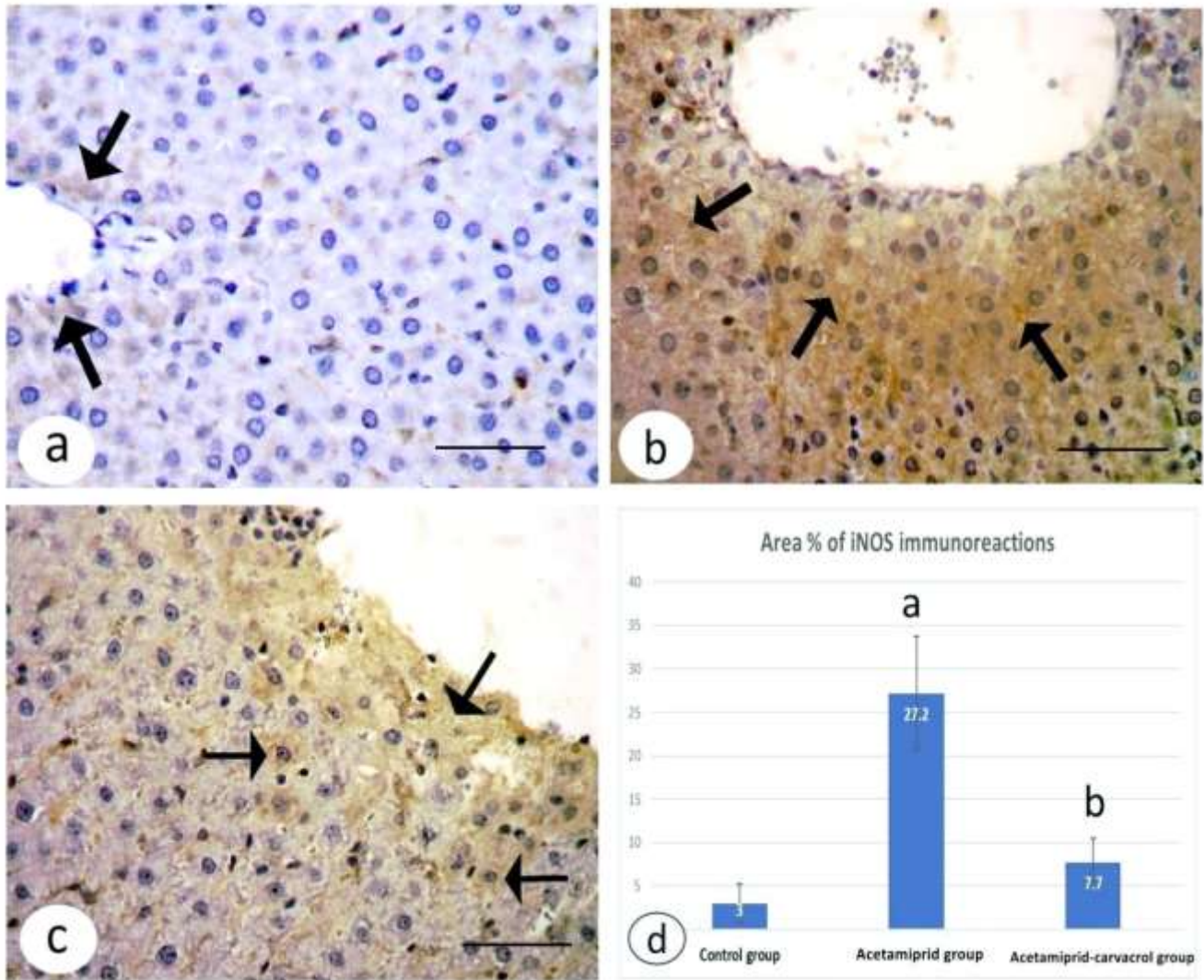


Figure 10: iNOS immunohistochemical reaction in liver Sections of different studied groups showing: Negative control group (a) shows weak positive cytoplasmic iNOS reaction in few hepatocytes (arrows). Acetamiprid group (b) shows strong positive iNOS reaction in most of the hepatocytes (arrows). Carvacrol +Acetamiprid group (c) shows mild positive iNOS reaction in some hepatocytes (arrows) (Immune peroxidase technique for iNOS x 400, scalebar 40µm). d. Comparison between area % of iNOS immunoreactions in different studied groups, a high significant difference with negative control group, b high significant difference with Acetamiprid group.

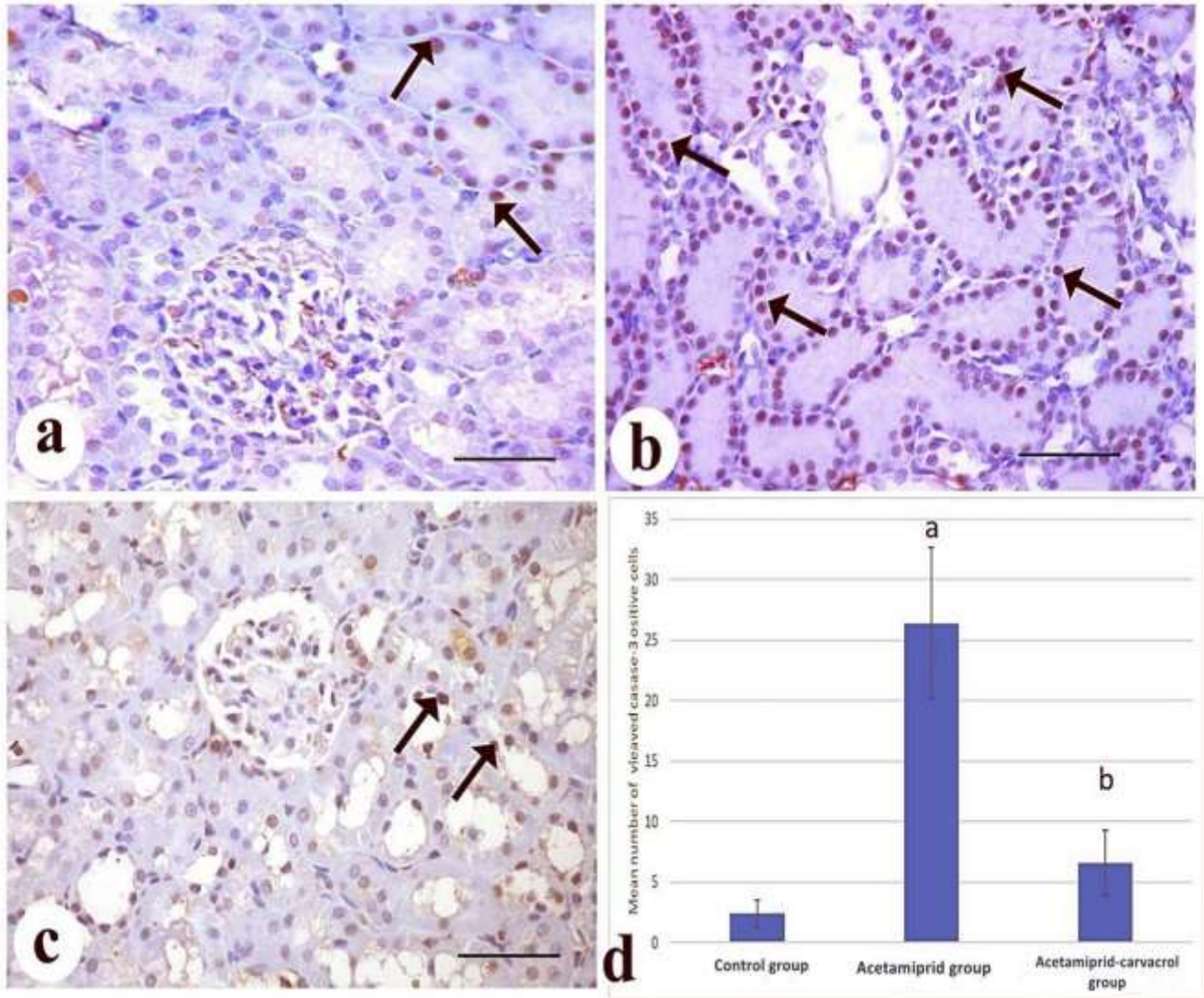


Figure 11: Sections of different studied groups showing cleaved caspase-3 immunohistochemical reaction: Negative control group (a) shows few cleaved caspase3 positive nuclei in few tubules (arrows). Acetamipride group (b) shows numerous cleaved caspase-3 positive nuclei in most renal tubules (arrows). Carvacrol+ Acetamipride group (c) shows some positive cleaved caspase3 nuclei among some tubules (arrows) (Immune peroxidase technique for cleaved caspase-3 x 400, scalebar 40µm). d. Comparison between mean number of cleaved caspase-3 positive cells in different studied groups, a high significant difference with negative control group, b high significant difference with Acetamiprid group.

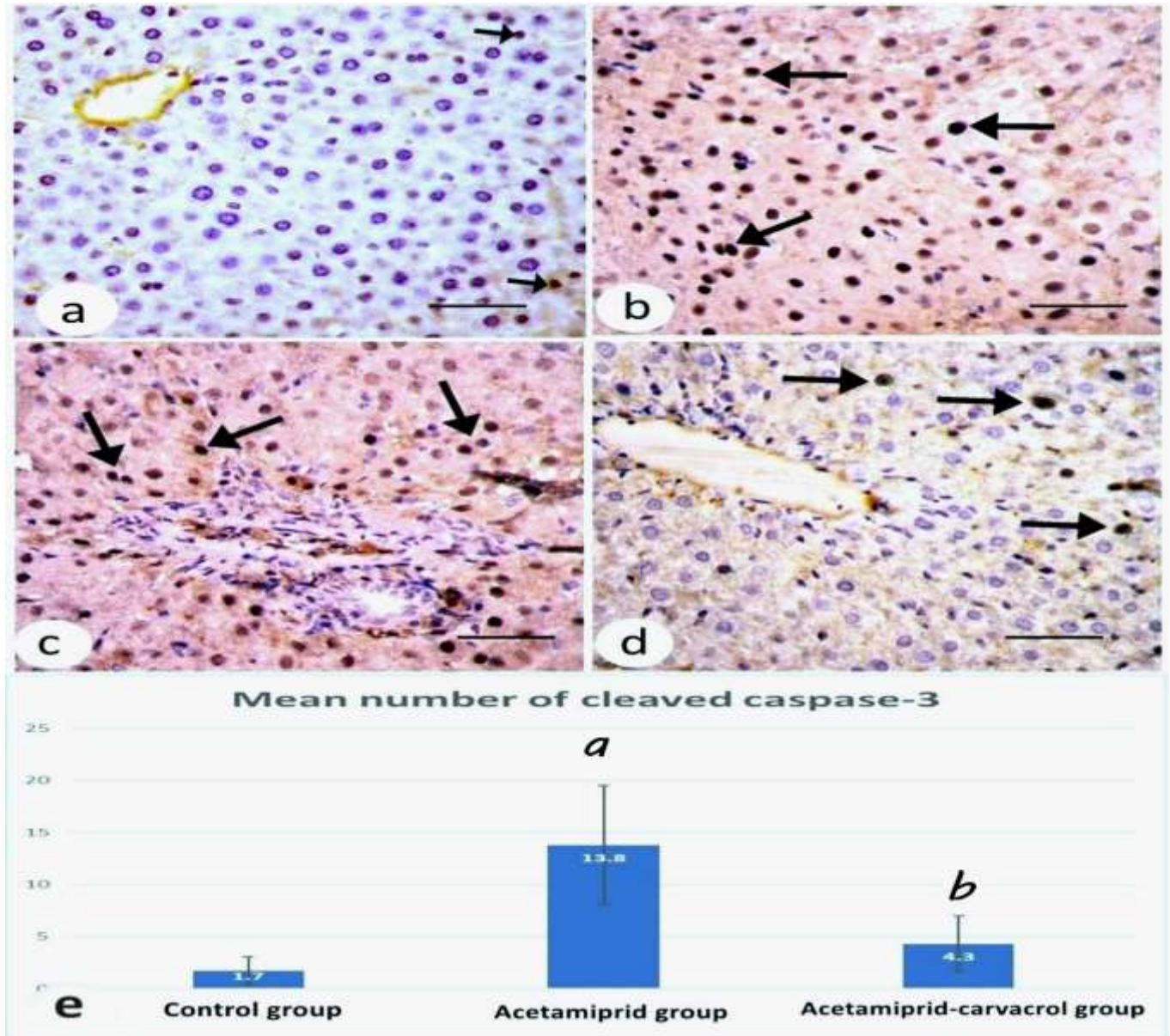


Figure12: Sections stained with cleaved caspase-3 of different studied groups showing: negative control group(a) shows few hepatocytes nuclei with positive cleaved caspase-3 immune reaction (arrows). Acetamidrid group(b,c) shows numerous nuclei with positive immune reaction to cleaved caspase-3 in most hepatocytes (arrows). Carvacrol +Acetamidrid- group(d) shows some positive cleaved caspase3 nuclei among some hepatocytes(arrows) (Immune peroxidase technique for cleaved caspase-3 x 400, scalebar 40µm). e. Comparison between mean number of cleaved caspase-3 positive cells in different studied groups, a high significant difference with control group, b high significant difference with Acetamidrid group

### III. DISCUSSION

Acetamiprid group showed statistically increase in urea, creatinine and uric acid serum level indicating alteration of renal function. The results of the current study demonstrate that Acetamiprid produced free radicals bind covalently to DNA and protein, resulting in the peroxidative destruction of lipid membranes.

Acetamiprid toxicity caused advanced liver damage, such as necrosis, enlarged sinusoidal space, cell accumulations and the infiltration of inflammatory cells into liver parenchyma. Aminotransferases which are highly sensitive, are thought to indicate damage to the liver's tissue. These enzymes leak from cytoplasm of liver cells and discharge into the blood due to increased permeability of membrane (*Adaramoye et al., 2008*). Consequently, elevation of these enzymes indicates hepatic cell injury, which is consistent with our histological findings and other studies (*Zhang et al., 2011, Mohany et al., 2012, Chakroun et al., 2016*).

Our study reported that exposure of rats to Acetamiprid reflected high level of lipid peroxidation parameter (MDA), while reduced glutathione and catalase enzyme, which have anti-oxidant activity showed lower level in Acetamiprid treated group than control group in both hepatic and renal tissues. Also gel electrophoresis revealed DNA laddering in

Acetamiprid treated group and this reflect presence of DNA damage.

Acetamiprid is absorbed into the tissues with ease. It interferes as a mutagen and potentially alters gene expression, both of which have the potential to cause cellular apoptosis. Pro- and anti-apoptotic proteins control apoptosis, which is planned cell death. Three main factors are DNA damage, oxidative stress, and changed gene expression, which can trigger intrinsic apoptosis (*Phogat et al., 2022*). Our study found that Acetamiprid treated group showed increased expression of P53 and Bax but decreased Bcl-2 gene expression in liver and kidney tissues. P53 is known as the "guardian of the genome" as it has the ability to cause apoptosis in cells by upregulating Bax and inhibiting Bcl-2 expression through both intrinsic and extrinsic pathways in the mitochondria (*Chen et al., 2010*).

According to *Gomez et al. (2020)*, Acetamiprid (1, 10 and 100  $\mu\text{M}$ ) treatment of trophoblast cells resulted in decreased cellular viability, up-regulated expression of Bax and down-regulated expression of Bcl-2. These changes were consistent with the current results.

Hematoxylin and eosin stained kidney section of acetamiprid group showing disturbed histological structure of renal cortex; the glomeruli are congested with obliteration of

bowman's space and the tubules had deep acidophilic cytoplasm and shredded cellular debris in their lumen which was in agreement with *Zhang et al. (2012)*. According to research by *Pasalic et al. (2012)*, the body's Uric Acid (UA) has the highest concentration of antioxidants, and the amount of UA in the serum is a crucial indicator of the body's anti-oxidation capacity. Acetamiprid reduced UA's activity. The relative rise of ROS that would result from a decrease in uric acid levels would inevitably cause an increase in the amount of NO production (*Robinson et al., 2011*).

NO production started a sequence of events that finally destroyed tubular epithelial cells and resulted in acute renal failure. In line with earlier findings that suggested NO may be involved in the acetamiprid-induced dysfunction of the kidney in mice (*Ruan et al., 2015*).

Kidney section from acetamiprid group stained by H&E revealing severe inflammatory cellular infiltration which agreed with *Erdemli et al. (2020)*. In current research, H&E-stained kidney section of acetamiprid group presented with massive interstitial haemorrhage, marked degenerative changes and areas of complete tissue necrosis are obvious which were in accordance with (*Noaishi and Abd Alhafez, 2016; Nur et al., 2022*).

Depletion of antioxidant levels may be the

cause of organ toxicity resulting from oxidative stress evolution during acetamiprid exposure, according to multiple research (*Erdemli et al. 2020, Khovarnagh and Seyedalipour 2021*). According to *Nur et al. (2022)*, exposure to acetamiprid dramatically enhanced protein and lipid oxidation by production of free radicals causing membrane proteins and lipids damage which leads to loss of cellular function.

*Rasgele et al. (2015)* explained mitochondrial dysfunction by Inhibition of fatty acid beta-oxidation, respiratory enzymes inhibition, and a direct effect on mitochondrial DNA are the three possible mechanisms by which it can happen. Some substances, such as pesticides, block the activity of respiratory enzymes as well as beta-oxidation. As a result of free fatty acids not being metabolized, lactate and reactive oxygen species accumulate generated. These radicals ultimately destroy the mitochondrial DNA after that.

In the current work, hepatocytes lost their normal arrangement and showed extensive vacuolations with dark stained nuclei which was consistent with *Phogat et al.'s (2020)* explanation that these histological abnormalities were caused directly by inflammation.

In this work, inflammatory cellular infiltrations and bile ducts proliferation were in agreement with *Noaishi and Abd Alhafez,*

(2016). According to *Mondal et al. (2014)*, rats given 25 mg/kg of Acetamiprid showed mild degenerative alterations in their liver.

In this study acetamiprid group exhibits increased collagen fibers deposition around blood vessels, renal tubules, the central vein, between hepatocytes, and in the portal region, which is like a study done by *Toghan et al. (2022)*.

An identifiable widespread fibrotic factor, TGF- $\beta$ , is crucial for the stimulation of fibroblasts, their differentiation, and the production of fibrotic matrix during tissue repair. Repeated kidney injury enhances TGF- $\beta$ -activity, which leads to aberrant ECM component formation, renal tissue replacement with fibrotic matrix, a progressive loss of glomerular filtration, and ultimately kidney failure. TGF- $\beta$  is the most important factor of epithelial mesenchymal transition (EMT) (*Meng et al. 2016; saifi et al. 2021*).

The acetamiprid group exhibits a strong positive iNOS reaction in several renal tubules in the current research, which was consistent with *Seemann et al. (2017)* findings. In line with *Erdemli et al. (2020)*, the acetamiprid group in the present research exhibits a significant cleaved caspase-3 positive nuclei in the majority of renal tubules.

The acetamiprid group in the current

research exhibits increased cleaved caspase-3 positive nuclei number and strong positive iNOS reaction in the majority of hepatocytes which was in agreement with (*Abdou et al. 2019*).

*El-Bialy et al. (2020)* reported that rats exposed to insecticides displayed increased levels of the apoptotic protein caspase-3 in hepatic and renal tissue.

Reactive oxygen species (ROS) production resulting in apoptosis may be connected to the elevation of caspase-3 expression in hepatic and renal tissues of inebriated rats. Prolonged exposure of rats to low concentrations of H<sub>2</sub>O<sub>2</sub> results in ROS production that activate caspase-3 and PKC $\delta$ , which induces nuclear DNA damage (*Carvour et al., 2008*). Caspase-3 oversees oxidative stress-induced apoptotic cell death. Additionally, insecticide induced oxidative stress in rats increased the protein expression of iNOS in hepatic and renal tissue, which may have contributed to hepatonephrotoxicity and injuries. It has been shown that pesticide intoxication increases iNOS production and caspase-3 gene expression (*Duzguner and Erdogan, 2012*).

Carvacrol reduces cyclophosphamide-induced renal damage and enhances kidney histology (*Gunes et al. 2017*). Also, *El-Sayed et al. (2015)* demonstrated that carvacrol mitigates cisplatin-induced kidney impairment by

decreasing glomerular and tubular necrosis.

In agreement with *Najafizadeh et al. (2022)*, in our present work most of the tubules appear to be normal in carvacrol+acetaminophen group, while there are still a few minor vacuolations and a few dark nuclei. Interstitial hemorrhage and residual mild glomerular congestion are also still present. Through its hydroxyl group, carvacrol has a strong antioxidant activity (*Suganthi and Manpal, 2013*). Additionally, it has been noted that the ischemia-reperfusion model's oxidative stress-induced kidney damage is inhibited by carvacrol (*Gheitasi et al. 2020*).

In our research, the carvacrol +acetaminophen group demonstrated improvement in the histological structure of the portal area, along with duct proliferation that was still evident and minimal cellular infiltration. With the exception of a few darkly stained nuclei, most hepatocytes appear normal. These data are like (*Ali et al., 2019*) who claimed that to considerable suppression effect of carvacrol on inflammatory markers. According to *Gholijani et al. (2015)*, thymol and carvacrol may improve the antioxidant defense mechanism and raise the activities of self-antioxidant enzymes.

The current study's carvacrol +acetaminophen group shows a minimal deposition of collagen fibers surrounding tubules and glomeruli, which is consistent with *Ram et al. (2022)* and mild

deposition of collagen fibers around central vein and in the portal area, which is consistent with *Zhao et al. (2021)*. Oral treatment of carvacrol resulted in decrease TGF- $\beta$  levels and Smad2/3 phosphorylation, according to *Ram et al. (2022)*. In addition, after carvacrol treatment, the elevated interstitial expression of collagens, fibronectin, and  $\alpha$ -SMA reduced.

Carvacrol inhibited the progression of rat liver fibrosis caused by carbon tetrachloride; this was linked to the Hippo and TGF- signaling pathways (*Mohseni et al., 2019*). Carvacrol had anti-fibrotic effect against TAA-induced hepatic fibrosis through decrease in hepatic TGF-  $\beta$ 1 content and a decrease in  $\alpha$ -SMA expression in the liver (*El-Gendy et al. 2021*).

In agreement with *Najafizadeh et al. (2022)*, the carvacrol +acetaminophen group from the current investigation exhibits some positive cleaved caspase3 nuclei among some tubules. They stated that high doses of acetaminophen can start the apoptosis cascade by overexpressing identified cleaved caspase-3 and Bax proteins in renal tissue as opposed to anti-apoptotic Bcl-2 protein. According to their findings, carvacrol may hinder kidney tissue from developing acetaminophen-induced apoptotic indicators.

*Khalaf et al. (2022)*, claimed that carvacrol decreased the level of iNOS mRNA expression.

In the present study, In acetamidrid-carvacrol group exhibits mild positive iNOS reaction in renal tubules and hepatocytes. carvacrol reduced NO production by preventing iNOS genes transcription mild positive iNOS reaction in some hepatocytes. carvacrol prevents the phosphorylation of mitogen-activated protein kinase (MAPK), which is essential for controlling cellular growth. When this protein is phosphorylated, it stimulates the activation of NF-kB, which triggers inflammatory cytokines IL-1b and iNOS release. carvacrol is considered a hepatoprotective substance due to its anti-inflammatory effects (*Khan et al. (2019)*).

#### IV. Conclusions

Administration of carvacrol produced partial and incomplete improvement of liver and kidney function and histology beside an improvement in oxidative stress and inflammation and DNA fragmentation caused by acetamidrid.

#### V. Recommendations

- Improving health education programs to raise public awareness about the danger of chemicals and pesticides like acetamidrid and its harmful effects in agricultural uses.

#### VI. Declaration and Statement

##### Availability of Data

The data used during the present research are available from the corresponding author upon reasonable request.

##### Financial Disclosures

This study was not reinforced by any source of funding.

##### Conflict of Interest

The authors encountered no conflict of interest.

##### Ethical Approval

Consent from the Zagazig University IACUC Committee in Egypt and in compliance with international rules for animal research (ZU-IACUC/3 F/42/2023).

#### VII. References

Assessment of the hepato-protective effect of developed lipid-polymer hybrid nanoparticles (LPH NPs) encapsulating naturally extracted  $\beta$ -Sitosterol against CCl<sub>4</sub> induced hepatotoxicity in rats. Scientific reports. 9(1),1-14. <https://doi.org/10.1038/s41598-019-56320-2>.

Adaramoye, O.; Ogungbenro, B.; Anyaegbu, O. et al. (2008): Protective effects of extracts of Vernonia amygdalina, Hibiscus sabdariffa and vitamin C against radiation-induced liver damage in rats. Journal of Radiation Research. 49(2), 123-131. <https://doi.org/10.1269/jrr.07062>.

Aebi, H. (1984): Methods in Enzymology.66,105:121-126. [https://doi.org/10.1016/S0076-6879\(84\)05016-3](https://doi.org/10.1016/S0076-6879(84)05016-3).

Ali, S; Khalifa, H. and Yousef, A. (2019): Protective effect of thymol and carvacrol on gentamycin-induced oxidative stress in male Albino rat. Benha Veterinary Medical

- Journal, 37(1), 204-209. <https://doi.org/10.21608/bvmj.2019.18064.1112>.
- Ahmadi , M.; Eidi,A.; Ahmadvand,H. et al.(2023): Effect of Carvacrol on histological analysis and expression of genes involved in an animal model of multiple sclerosis. *Multiple Sclerosis and Related Disorders*. 70, 104471. <https://doi.org/10.1016/j.msard.2022.104471>.
- Arigesavan, K., & Sudhandiran, G. (2015). Carvacrol exhibits anti-oxidant and anti-inflammatory effects against 1, 2-dimethyl hydrazine plus dextran sodium sulfate induced inflammation associated carcinogenicity in the colon of Fischer 344 rats. *Biochemical and Biophysical Research Communications*. 461(2), 314–320. <https://doi.org/10.1016/j.bbrc.2015.04.030>.
- Arora, D.; Siddiqui, M.; Sharma, P. et al. (2016): Deltamethrin induced RIPK3-mediated caspase-independent non-apoptotic cell death in rat primary hepatocytes. *Biochemical Biophysical Research Community*. 479:217-223. <https://doi.org/10.1016/j.bbrc.2016.09.042>.
- Azouz, R. and Korany, R. (2020): Toxic impacts of amorphous silica nanoparticles on liver and kidney of male adult rats: an in vivo study. *Biological Trace Element Research*. 199: 2653-2662. <https://doi.org/10.1007/s12011-020-02386-3>.
- Bancroft, J. and Gamble, M. (2008): *Theory and Practice of Histological Techniques*. 6th ed., Churchill Livingstone, New York, Edinburgh, London.18, 165-175.
- Banik, S., Akter, M., Bondad, S. et al. (2019): Carvacrol inhibits cadmium toxicity through combating against caspase dependent/independent apoptosis in PC12 cells. *Food and Chemical Toxicology*. 134, 110835. <https://doi.org/10.1016/j.fct.2019.110835>.
- Carvour, M.; Song, C.; Kaul, S.; et al. (2008): Chronic low-dose oxidative stress induces caspase-3-dependent PKCdelta proteolytic activation and apoptosis in cell culture model of dopaminergic neurodegeneration. *Ann N Y Acad Sci*. 1139:197-205. <https://doi.org/10.1196/annals.1432.020>.
- Chakroun, S.; Ezzi, L.; Grissa, I. et al. (2016): Hematological, biochemical, and toxicopathic effects of subchronic acetamiprid toxicity in Wistar rats. *Environmental Science and Pollution Research*, 23, 25191-25199. <https://doi.org/10.1007/s11356-016-76509>.
- Chauhan, K.; Kanani, D.; Patel, P. et al. (2017): Serum creatinine: conventional and compensated kinetic method with enzymatic

- method. *International Journal of Clinical Biochemical Research*. 4(2): 206-209. <https://api.semanticscholar.org/CorpusID:212598343>.
- Chen, H.; Bi.W.; Cao, B. et al. (2010): novel podophyllotoxin derivative (YB-1EPN) induces apoptosis and down-regulates express of P-glycoprotein in multidrug resistance cell line KBV200. *European journal of pharmacology*. 627 (1-3): 69–74. <https://doi.org/10.1016/j.ejphar.2009.06>
- Eftekhari, A.; Hasanzadeh, A.; Khalilov, R. et al (2020): Hepatoprotective role of berberine against paraquat-induced liver toxicity in rat. *Environmental Science and Pollution Research* 27:4969–4975. <https://doi.org/10.1007/s11356-019-07232-1>.
- Egwurugwu, J.; Ohamaeme, M.; Ekweog, C. et al. (2018): Effects of Formalin inhalation on physical characteristics and renal profile of albino wistar rats. *Asian Journal of Medicine and Health*. 12(4): 1-11. <http://dx.doi.org/10.9734/AJMAH/2018/44412>.
- Duzguner, V. and Erdogan, S. (2012): Chronic exposure to imidacloprid induces inflammation and oxidative stress in the liver & central nervous system of rats. *Pesticide Biochemical Physiology* .104:58-64. <https://doi.org/10.1016/j.pestbp.2012.06.01>
- El- Bialy, B.; Abd Eldaim, M.; Hassan, A. et al. (2020): Ginseng aqueous extract ameliorates lambda- cyhalothrin- acetamiprid insecticide mixture for hepatorenal toxicity in rats: role of oxidative stress- mediated proinflammatory and proapoptotic protein expressions. *Environmental toxicology*.35(2), 124-135. <https://doi.org/10.1002/tox.22848>.
- El-Gendy, Z.; Ramadan, A.; El-Batran, S. et al. (2021): Carvacrol hinders the progression of hepatic fibrosis via targeting autotaxin and thioredoxin in thioacetamide-induced liver fibrosis in rat. *Human & Experimental Toxicology*. 40 (12), 2188-2201. <https://doi.org/10.1177/096032712111026729>.
- El-Sayed, E.; Abd-Allah, A.; Mansour, A. et al. (2015): Thymol and carvacrol prevent cisplatin-induced nephro-toxicity by abrogation of oxidative stress, inflammation, and apoptosis in rats. *Journal of Biochemistry and Molecular Toxicology* .29(4):165–172. <https://doi.org/10.1002/jbt.21681>.
- Erdemli, M.; Zayman, E.; Erdemli, Z.; et al (2020): Protective effects of melatonin and vitamin E in acetamiprid-induced nephrotoxicity. *Environment Science and Pollution Research* 27:9202-9213. <https://doi.org/10.1007/s11356-019->

06754-y.

Gheitasi, I.; Azizi, A.; Omidifar, N. et al. (2020): Renoprotective effects of Origanum majorana methanolic L and carvacrol on ischemia/reperfusion-induced kidney injury in male rats. Evidence Based Complement Alternative Medicine . 1-9.

<https://doi.org/10.1155/2020%2F9785932>.

Gholijani, N.; Gharagzloo, M.; Kalantar, F. et al. (2015): Modulation of cytokine production and transcription factors activities in human Jurkat T cells by thymol and carvacrol. Advanced pharmaceutical bulletin. 5(1): 653. <https://doi.org/10.1517/apb.2015.089>.

Gomez, S.; Bustos, P.; Sánchez, V. et al. (2020): Trophoblast toxicity of the neonicotinoid insecticide acetamiprid and an acetamiprid-based formulation. Toxicology, 431: 152363. <https://doi.org/10.1016/j.tox.2020.152363>.

Gunes, S.; Ayhanci, A.; Sahinturk, V. et al. (2017): Carvacrol attenuates cyclophosphamide-induced oxidative stress in rat kidney. Canadian Journal of Physiology and Pharmacology. 95(7):844–849. <https://doi.org/10.1139/cjpp-2016-0450>.

Gu, Y. ; Liu, X. ; Huang, X. . et al. (2020): Diverse role of TGF- $\beta$  in kidney disease.

Frontiers in cell and developmental biology, 8,

123.

<https://doi.org/10.3389/fcell.2020.00123>.

Iwakiri, Y. and Kim, M. (2015): Nitric oxide in liver diseases. Trends in Pharmacological Science. <https://doi.org/10.1016/j.tips.2015.05.001>.

Javed,H. ; Meeran,M. and Jha,N. (2021): Carvacrol, a Plant Metabolite Targeting Viral Protease (Mpro) and ACE2 in Host Cells Can Be a Possible Candidate for COVID-19. Frontier In Plant Science.36(8):524-536. - <https://doi.org/10.3389/fpls.2020.601335>.

Karaca, B. ; Arican, Y. ; Boran, T. et al (2019): Toxic effects of subchronic oral acetamiprid exposure in rats. Toxicology Indian Health 35:679–687. <https://doi.org/10.1177/0748233719893203>.

Khalaf, A.; Hassanen, E. and Azouz, R. (2019): Ameliorative effect of zinc oxide nanoparticles against dermal toxicity induced by lead oxide in rats. International journal of nano-medicine; 14:7729-7741. <https://doi.org/10.2147/ijn.s220572>.

Khalaf, A., Elhady, M.; Hassanen ,E. et al. (2021): Antioxidant role of carvacrol against hepatotoxicity and nephrotoxicity induced by propiconazole in rats. Revista Brasileira de Farmacognosia. 31: 67-74.

<https://doi.org/10.1007/s43450-021-00127-8>.

- Khalaf, M.; Hassan, S.; Sayed, A. et al. (2022): Carvacrol mitigates vancomycin-induced nephrotoxicity via regulation of I $\kappa$ B $\alpha$ /p38MAPK and Keap1/Nrf2 signaling pathways: an experimental study with in silico evidence. *European Rev Medical Pharmacology Science*, 26(23), 8738-8755. [https://doi.org/10.26355/eurrev.202212\\_30546](https://doi.org/10.26355/eurrev.202212_30546).
- Khan, I.; Bhardwaj, M.; Shukla, S. et al. (2019): Carvacrol inhibits cytochrome P450 and protects against binge alcohol-induced liver toxicity. *Food and Chemical Toxicology*. 131, 110582. <https://doi.org/10.1016/j.fct.2019.110582>.
- Khovarnagh, N. and Seyedalipour, B. (2021): Antioxidant, histopathological and biochemical outcomes of short-term exposure to acetamiprid in liver and brain of rat: The protective role of N-acetylcysteine and S-methylcysteine. *Saudi Pharmaceutical Journal*. 29:280-289. <https://doi.org/10.1016/j.jsps.2021.02.004>.
- Maalej, A.; Mahmoudi, A.; Bouallagui Z. et al. (2017): Olive phenolic compounds attenuate deltamethrin-induced liver and kidney toxicity through regulating oxidative stress, inflammation and apoptosis. *Food and chemical toxicology*. 106: 455-465. <https://doi.org/10.1016/j.fct.2017.06.010>.
- Mahmoodi, M. Amiri, H. Ayoobi, F. et al. (2019): Carvacrol ameliorates experimental autoimmune encephalo-myelitis through modulating pro- and anti-inflammatory cytokines. *Life Sciences*. 219. 257-263. <https://doi.org/10.1016/j.lfs.2018.11.051>.
- Mannervik, B. (1999): Measurement of glutathione reductase activity. *Current Protocols in Toxicology*; (1): 7-2. <https://doi.org/10.1002/0471140856.tx0702.s00>.
- Masyita, A.; Sari, R.; Astuti, A. et al. (2022): Terpenes and terpenoids as main bioactive compounds of essential oils, their roles in human health and potential application as natural food preservatives. *Food Chemistry*: 13.100217. <https://doi.org/10.1016/j.fochx.2022.100217>.
- Meng, X.; Nikolic-Paterson, D. and Lan, H. (2016): TGF- $\beta$ : the master regulator of fibrosis. *Nature Reviews Nephrology*. 12(6):325-338. <https://doi.org/10.1038/nrneph.2016.48>.
- Mondal, S.; Ghosh, R.; Karnam, S. et al. (2014): Toxicopathological changes on Wistar rat after multiple exposures to acetamiprid. *Veterinary world*. 7(12): 1058-

1065. <http://dx.doi.org/10.14202/vetworld.2014.1058-1065>.
- Mohseni, R.; Karimi, J.; Tavilani, H. et al. (2019): Carvacrol ameliorates the progression of liver fibrosis through targeting of Hippo and TGF  $\beta$  signaling pathways in carbon tetra chloride (CCl<sub>4</sub>) induced liver fibrosis in rats. *Immunopharmacology and Immunotoxicology*. 41: 163- 171. <https://doi.org/10.1080/08923973.2019.1566926>.
- Najafizadeh, A.; Kaeidi, A.; Rahmani, M. et al. (2022). The protective effect of carvacrol on acetaminophen-induced renal damage in male rats. *Molecular Biology Reports*. 49(3), 1763-1771. <https://doi.org/10.1007/s11033-021-06985-8>.
- Noaishi, M. A. and Abd Alhafez, H. H. (2016): Hepatotoxicity and nephrotoxicity evaluation after repeated dose of acetamiprid in albino rats. *Egyptian Journal of Chemistry and Environmental Health*. 2(2), 439-452. <https://doi.org/10.21608/ejceh.2016.254597>.
- Nur, G.; Caylak, E.; Kilicle, P. et al. (2022). Immunohistochemical distribution of Bcl-2 and p53 apoptotic markers in acetamiprid-induced nephrotoxicity. *Open Medicine*, 17(1): 1788-1796. <https://doi.org/10.1515/med-2022-0603>.
- Ohkawa, H.; Ohishi, N. and Yagi, K. (1979): Assay for lipid peroxides in animal tissues by thiobarbituric acid reaction. *Annual. Biochemistry*. 95 (2): 351- 358. [https://doi.org/10.1016/0003-2697\(79\)90738-3](https://doi.org/10.1016/0003-2697(79)90738-3).
- Pasalic, D.; Marinkovic, N. and Feher-Turkovic, L. (2012): Uric acid as one of the important factors in multifactorial disorders-facts and controversies. *Biochemical. Medic-ine*, 22: 63-75. <https://doi.org/10.11613/bm.2012.007>.
- Phogat, A.; Singh, J.; Kumar, V. et al. (2022): Toxicity of the acetamiprid insecticide for mammals: A review. *Environmental Chemistry Letters*; 1-26. <https://doi.org/10.1007/s10311-021-01353-1>.
- Phogat, A.; Singh, J.; Kumar, V. et al. (2023): Berberine mitigates acetamiprid induced hepatotoxicity and inflammation via regulating endogenous antioxidants and NF- $\kappa$ B/TNF- $\alpha$  signaling in rats. <https://doi.org/10.1007/s11356-023-28279-1>.
- Ram, C.; Gairola, S.; Syed, A. et al. (2022): Carvacrol preserves antioxidant status and attenuates kidney fibrosis via modulation of TGF- $\beta$ 1/ Smad signaling and inflammation. *Food & Function*, 13(20): 10587-10600. <https://doi.org/10.1039/d2fo01384c>.

- Rasgele, P.; Oktay, M.; Kekecoglu, M. et al. (2015): The histopathological investigation of liver in experimental animals after short-term exposures to pesticides. *Bulgarian Journal of Agricultural Science*. 21 (2): 446–453.
- Reitman, S. and Frankel, S. (1957): A colorimetric method for the determination of serum glutamic oxalacetic and glutamic pyruvic transaminases. *American Journal of Clinical Pathology*. 28(1): 56-63. <https://doi.org/10.1093/ajcp/28.1.56>.
- Robinson, M.; Baumgardner, J. and Otto, C. (2011): Oxygen-dependent regulation of nitric oxide production by inducible nitric oxide synthase. *Free Radical Biology Medicine*. 51: 1952-1965. <https://doi.org/10.1016/j.freeradbiomed.2011.08.034>.
- Rosa, S.; Goncalves, J.; Judas, F. et al (2009): Impaired glucose transporter-1 degradation and increased glucose transport and oxidative stress in response to high glucose in chondrocytes from osteoarthritic versus normal human cartilage. *Arthritis Research Therapy*. 11, 80.
- Ruan, S.; Huang, T.; Wu, H. et al. (2015): Inhaled nitric oxide therapy and risk of renal dysfunction: a systematic review and meta-analysis of randomized trials. *Critical Care*. (19):1. <https://doi.org/10.1186/s13054-015-0880-2>.
- Samarghandian, S.; Farkhondeh, T.; Samini, F. et al. (2015): Protective Effects of Carvacrol against Oxidative Stress Induced by Chronic Stress in Rat's Brain, Liver, and Kidney. *Biochemistry Research International*. Article ID 2645237, 7. <http://dx.doi.org/10.1155/2016/2645237>.
- Saifi, M.; Annaldas, S. and Godugu, C. (2021): A direct thrombin inhibitor, dabigatran etexilate protects from renal fibrosis by inhibiting protease activated receptor-1. *European Journal of Pharmacology*, 893, 173838. <https://doi.org/10.1016/j.ejphar.2020.173838>.
- Seemann, S.; Zohles, F. and Lupp, A. (2017): Comprehensive comparison of three different animal models for systemic inflammation. *Journal of Biomedical Science*. 24(1):1–7. <https://doi.org/10.1186/s12929-017-0370-8>.
- Sevim, Ç.; Akpınar, E.; ASksu, E. ; . et al. (2023): Reproductive effects of s. boulardii on sub-chronic acetamiprid and imidacloprid toxicity in male rats. *Toxics*, 11, 170. <https://doi.org/10.3390/toxics11020170>.
- Sinha, A. K. (1972): Colorimetric assay of

- catalase. *Analytical Biochemistry*; 47(2): 389-394. [https://doi.org/10.1016/0003-2697\(72\)90132-7](https://doi.org/10.1016/0003-2697(72)90132-7).
- Siniscalco, D.; Trotta, M.; Brigida, A. et al. (2018): Intraperitoneal administration of oxygen/ozone to rats reduces the pancreatic damage induced by streptozotocin. *Biology*. 7(1):10-16. <https://doi.org/10.3390/biology7010010>.
- Suganthi, R. and Manpal, S. (2013): Biological and pharmacological of actions carvacrol and its effects on poultry: an updated review. *World Journal of Pharmacology Science*. 2:3581–3595.
- Suvarna, K. Layton, C. and Bancroft, J. (2018): Bancroft's Theory and Practice of Histological Techniques E-Book. Oxford: Elsevier Health Sciences; 27.
- Sternberger, L. (1986): *Immunocytochemistry*. 3rd Ed. New York: John Wiley Medical; 524.
- Toghan, R.; Amin, Y. ; Ali, R. . et al. (2022): Protective effects of Folic acid against reproductive, hematological, hepatic, and renal toxicity induced by Acetamiprid in male Albino rats. *Toxicology*, 469, 153115. <https://doi.org/10.1016/j.tox.2022.153115>.
- Yan, S.; Meng, Z.; Tian, S. et al. . (2020): Neonicotinoid insecticides exposure cause amino acid metabolism disorders, lipid accumulation and oxidative stress in ICR mice. *Chemosphere* 246:125661. <https://doi.org/10.1016/j.chemosphere.2019.125661>.
- Zhao, W.; Chen, L.; Zhou, H. et al. (2021): Protective effect of carvacrol on liver injury in type 2 diabetic db/db mice. *Molecular Medicine Reports*, 24(5), 1-11. <https://doi.org/10.3892/mmr.2021.12381>.
- Zhang, J.; Wang, Y.; Xiang, H. et al. (2012): Nephrotoxicity of acetamiprid on male mice and the rescue role of vitamin E. *Journal of Animal and Veterinary Advances*, 11(15), 2721-2726. <https://doi.org/10.3923/JAVAA.2012.2721.2726>.
- Zhang,s.; Zhao, M.; Li,S. . et al. (2023): Developmental toxicity assessment of neonicotinoids and organophosphate esters with a human embryonic stem cell- and metabolism-based fast-screening model. *Journal of Environmental Sciences*. 137:370-381. <https://doi.org/10.1016/j.jes.2023.02.02>.

**How to cite:** Ibrahim, N., Assy, W., Mohamed, S., El-Mahroky, S., Sameh, H., Megahed, E. (2024). Evaluation of the Role of Carvacrol against Acetamiprid Induced Apoptosis and DNA Damage in Liver and Kidney of Adult Male Albino Rats. *Zagazig Journal of Forensic Medicine and Toxicology*, 22(2), 17-52. doi: 10.21608/zjfm.2024.269995.1177